

# **Corrosion study of anodes for magnesium air batteries**

**Eric Pla Erra**

Thesis to obtain the Master of Science Degree in  
**Energy Engineering and Management**

Supervisors: Prof. Maria de Fátima Grilo da Costa Montemor  
Prof. António Pedro dos Santos Lopes Castela

## **Examination Committee**

Chairperson: Prof. Francisco Manuel da Silva Lemos  
Supervisor: Prof. Maria de Fátima Grilo da Costa Montemor  
Member of the Committee: Prof. Maria Teresa Oliveira de Moura e Silva

**December 2019**



## Acknowledgements

In this brief section I would like to thank all the people in the electrochemistry lab at IST. Special thanks to professor Fátima Montemor, who supervised all the work, guided me through the process and gave her expert advice on the topic.

I would also like to give special thanks to Lenia Calado, who helped me a lot in the laboratory and without her help this thesis could not have happened.

This excellent opportunity was possible for me to be done thanks to Innoenergy, so I would like to thank all the effort this group of people is doing for the energy sector, the youth and the entrepreneurship in Europe.

Finally, I would like to appreciate all the support I have received from my family since the beginning, being far away from home for so long is not easy and they helped me through the few rough moments of the process.

## Abstract

This thesis aims at studying corrosion phenomena in magnesium alloys that can be used as anodes in magnesium air batteries, and how to possibly control it. A discussion on the main problem addressed as well as the definition of the dissertation objectives considering the state of the art and future for magnesium air batteries will be presented. After this, the methodology followed is introduced in the experimental section, with its main parts being sample preparation, equipment and techniques used. The experimental part of the dissertation project consists on the description of four electrochemical techniques that are used to characterize the corrosion processes at the Mg anode. These techniques will be used to study the anode response in blank electrolyte, an aqueous solution of  $\text{NaNO}_3$ . The same techniques will also be used to study the effect of an added inhibitor in the electrolyte in order to determine how the corrosion behavior changed and how this could benefit magnesium air batteries. Different concentrations were tested to find the most suitable one. The inhibitor used is sodium phosphate. The obtained results suggest that the usage of proper inhibitor concentration can increase the cell voltage but there is evidence of the formation of a resistive layer that creates unwanted diffusion overpotential and negative current response. Future work should include a larger range of inhibitors and concentrations and a cell setup to run extra discharge curves and to determine the cell capacity.

### **Key words**

Magnesium air battery; anode; corrosion; inhibitor; electrolyte

## Resumo

Esta tese tem como objetivo estudar e controlar os fenômenos de corrosão em ligas de magnésio que podem ser usadas como ânodos em baterias de magnésio ar. Será apresentada uma discussão sobre o principal problema abordado, bem como a definição dos objetivos da dissertação, considerando o estado da arte e o futuro das baterias de magnésio ar. Depois disso, descreve-se a metodologia, na seção experimental, nomeadamente detalhes relativos à preparação das amostras, ao equipamento e às técnicas utilizadas. A parte experimental do projeto de dissertação envolve a utilização de quatro técnicas eletroquímicas que foram utilizadas para caracterizar os processos de corrosão no ânodo Mg. Essas técnicas serão utilizadas para estudar a resposta eletroquímica dos ânodos no eletrólito de referência, uma solução aquosa de  $\text{NaNO}_3$ . Essas técnicas foram também usadas para estudar o efeito de um inibidor adicionado no eletrólito, a fim de determinar como a presença de inibidor afeta o comportamento face à corrosão do ânodo de Mg e como isso afeta a resposta da bateria de magnésio ar. O inibidor usado é o fosfato de sódio. Os resultados obtidos sugerem que o uso de uma concentração adequada de inibidor pode aumentar a voltagem da célula, mas há evidências da formação de uma camada resistiva que cria um potencial de difusão indesejável e uma resposta de corrente pouco eficiente. Trabalhos futuros devem incluir uma gama mais alargada de inibidores e concentrações e uma configuração de célula eletroquímica que permita obter curvas de descarga e determinar a capacidade da célula.

### **Palavras-chave**

Bateria de magnésio-ar; ânodo; corrosão; inibidor; eletrólito



## Table of figures

Figure 1 Energy density comparison between the most common used battery technologies in the market [6] .....	- 2 -
Figure 2 Lead Acid Battery components and main chemistry [7] .....	- 3 -
Figure 3 Simplified sealed NiCd design and chemical reactions [10] .....	- 4 -
Figure 4 NaS battery scheme [12] .....	- 4 -
Figure 5 Basic scheme of a Lithium ion battery [6] .....	- 5 -
Figure 6 Comparison of Battery Energy Storage Technologies [15] .....	- 6 -
Figure 7 Comparison of Voltage, Specific Energy and Volumetric Energy Density of metal air batteries [18] .....	- 7 -
Figure 8 Basic structure and chemistry of both aqueous and non aqueous metal air batteries [18] .....	- 7 -
Figure 9 Graphic visualization of the different layers found in a typical cathode of a metal air battery [20] .....	- 8 -
Figure 10 Basic structure and working principle of a Mg air battery [20] .....	- 12 -
Figure 11 Different types of magnesium alloys anode materials for Mg air batteries [20] .....	- 13 -
Figure 12 Rest potential of magnesium anode when immersed in different aqueous electrolytes [20] .....	- 14 -
Figure 13 Mg system vs. Li system [26] .....	- 16 -
Figure 14 Different electrolyte solutions comparison regarding cumulative H <sub>2</sub> evolution [28]. ...	- 18 -
Figure 15 Comparison of different inhibitor corrosion substances to improve performance of primary Mg cells [30] .....	- 20 -
Figure 16 Testing of a sample in the Reference Gamry 600+ .....	- 21 -
Figure 17 Gamry Reference 600+ .....	- 22 -
Figure 18 EIS results of pure magnesium samples in 3.5 wt% of NaCl solution. (a) Nyquist plots and (b) Bode plots. 3 samples of pure magnesium (99.95 wt.%) ingots are extruded at the temperatures of 180 °C, 200 °C, and 250 °C, respectively. [35]. .....	- 25 -
Figure 19 Anodic and Cathodic Polarization resistance curves using blank electrolyte. ....	- 27 -
Figure 20 Anodic and cathodic curves in the same graph using 0.05 M sodium phosphate..	- 29 -
Figure 21 Anodic and cathodic curves in the same graph using 0.01 M sodium phosphate..	- 30 -
Figure 22 Anodic and cathodic curves in the same graph using 0.005 M sodium phosphate..	- 31 -
-	
Figure 23 All anodic curves plotted together .....	- 32 -
Figure 24 Open Circuit Potential using blank electrolyte during the first 24 h of immersion	- 33 -
Figure 25 OCP on the 25th hour after immersion .....	- 34 -
Figure 26 24 h OCP with inhibitor .....	- 35 -
Figure 27 Optical comparison between the two samples .....	- 36 -
Figure 28 Impedance Nyquist plot using blank electrolyte .....	- 37 -
Figure 29 Impedance Bode plot using blank electrolyte .....	- 38 -
Figure 30 Nyquist plot using sodium phosphate as corrosion inhibitor .....	- 39 -
Figure 31 Bode plots using sodium phosphate as corrosion inhibitor .....	- 40 -
Figure 32 Galvanostatic discharge curves using blank electrolyte .....	- 43 -
Figure 33 Discharge curves at 2.5 mA using different inhibitor concentrations .....	- 44 -
Figure 34 Discharge curves at 5 and 10 mA .....	- 45 -
Figure 35 OCP first 600 seconds .....	- 51 -
Figure 36 OCP first hour .....	- 51 -

Figure 37. Impedance Nyquist plot sample 2..... - 51 -



## Contents

Acknowledgements.....	iii
Abstract.....	iv
Resumo.....	v
Table of figures.....	vii
Definition of the problem .....	- 1 -
1. Introduction .....	- 2 -
1.1. Electrochemical batteries.....	- 2 -
1.1.1. Lead acid.....	- 2 -
1.1.2. Nickel batteries .....	- 3 -
1.1.3. NaS batteries .....	- 4 -
1.1.4. Flow batteries.....	- 5 -
1.1.5. Lithium ion batteries .....	- 5 -
1.1.6. Metal air batteries.....	- 6 -
1.2. Mg Air batteries - State of the art .....	- 12 -
1.3. Future .....	- 16 -
2. Corrosion inhibitors for the Mg anodes .....	- 18 -
3. Methodology.....	- 21 -
3.1. Sample preparation.....	- 21 -
3.2. Equipment.....	- 22 -
3.3. Techniques .....	- 24 -
3.3.1. Open Circuit Potential .....	- 24 -
3.3.2. Electrochemical Impedance Spectroscopy.....	- 25 -
3.3.3. Potentiodynamic Polarization .....	- 25 -
3.3.4. Galvanostatic Discharge .....	- 26 -
4. Results and discussion.....	- 27 -
4.1. Potentiodynamic Polarization .....	- 27 -
4.1.1. Blank electrolyte results.....	- 27 -
4.1.2. Results with inhibitor .....	- 29 -
4.1.3. Comparison and discussion of the results.....	- 32 -
4.2. Open Circuit Potential .....	- 33 -
4.2.1. Blank electrolyte results.....	- 33 -
4.2.2. Results with inhibitor .....	- 35 -
4.2.3. Comparison and discussion of the results.....	- 36 -

4.3.	Electrochemical Impedance Spectroscopy .....	- 37 -
4.3.1.	Blank electrolyte results.....	- 37 -
4.3.2.	Results with inhibitor .....	- 39 -
4.4.	Galvanostatic Discharge .....	- 42 -
4.4.1.	Blank electrolyte results.....	- 42 -
4.4.2.	Results with inhibitor .....	- 44 -
5.	Conclusions .....	- 46 -
6.	Future work.....	- 47 -
7.	References.....	- 48 -
Annex	.....	- 51 -
A.1.	Open circuit potential .....	- 51 -



## Definition of the problem

Having a look at the World's Energy Outlook 2018, released by the International Energy Agency, it is observed that the world's energy demand is expected to increase almost 30% in the next twenty years. This is equivalent to an increase of almost 4 million tons oil equivalent (mtoe). This data corresponds to the New Policies Scenario (current and expected or announced policies).[1]

Renewable energies will play an important role in this energy demand increase. It is expected an increase of more than 80% in the period 2017-2040, where they will account for 20% of overall energy demand. [1]

The most important drawback of renewable energy sources is that they do not deliver energy in a continuous reliable way, which creates a big challenge to ensure stability in the supply. One of the proposed solutions to this problem consists on the use of electrochemical energy storage solutions such as batteries, which have been widely used as the best generation support technology mainly due to its portability and versatility in different applications. [2]

Lithium batteries are the most widespread batteries in both the primary and secondary markets. Lithium batteries present some drawbacks, like explosion risks in presence of moisture contamination and its high price, but its major drawback that is interesting for the development of this thesis is that Li is a scarce material and that this type of batteries are reaching the performance limits, triggering a global search for safer, cheaper and more efficient electrochemical energy storage technologies. [3]

Another important drawback related to lithium batteries is related to the use of cobalt. At a time when smartphones and electric cars set the tone, the vast cobalt reserves located in the subsoil of the Democratic Republic of the Congo are the object of greed by large multinationals with several environmental and social concerns. [4]

According to UNICEF, more than 40,000 children under 7 years old work in the mines of the Democratic Republic of the Congo. A Sky News report, released in February 2017, shows how young children work under very harsh conditions in Congolese cobalt mines, while Amnesty International has repeatedly denounced the deplorable conditions of child labor in the country. Citing this report, *"approximately 20% of the total cobalt production of the DRC is done by hand, children extract it using rudimentary tools and without any protection."*[4]

In conclusion, even though lithium batteries are the bread and butter of the new technological era, their drawbacks are pushing the scientific community to research and investigate different options to substitute them in a wide array of applications. Metal air batteries are emerging as interesting devices to fulfill both stationary and mobile applications. Magnesium is emerging an interesting alternative as anode material but still suffers of drawbacks such as corrosion susceptibility, a phenomenon that needs to be understood and controlled to extend anodes lifetime. Therefore, this thesis aims to study the corrosion activity and its inhibition on AZ31 used as anode in Magnesium Air batteries.

## 1. Introduction

The battery as we know it today was invented over 200 years ago by a scientist named Alessandro Volta [5]. There are two main types of batteries: primary and secondary. A primary cell is designed to be used only one time and it cannot be recharged, while secondary cells are designed to be electrically recharged many times during their lifetime. An electrochemical battery is able to store energy by holding certain electro-chemically active materials in the same cell setup. The battery main function is to generate and store electrons, which will be delivered when needed. Many technologies that are commonly used today are powered by batteries, including smartphones, computers and cars (both electric and conventional). Many battery families exist in the market. In addition to conventional lead acid batteries and modern Li ion batteries, metal air batteries are used in specific market niches such as mobility and military applications. [5]

### 1.1. Electrochemical batteries

The most important parts of an electrochemical battery are the two electrodes, one being negative (anode) and the other one being positive (cathode), a separator and the electrolyte which can be in both liquid and solid states and that ensures ionic transport and transports the ions from anode to cathode [5]. There is a wide range of different battery technologies, from robust lead acid batteries to more recent like lithium ion batteries. Each one of them has different attributes and applications [5]. Figure 1 shows how different energy densities are found between these commonly used battery types:

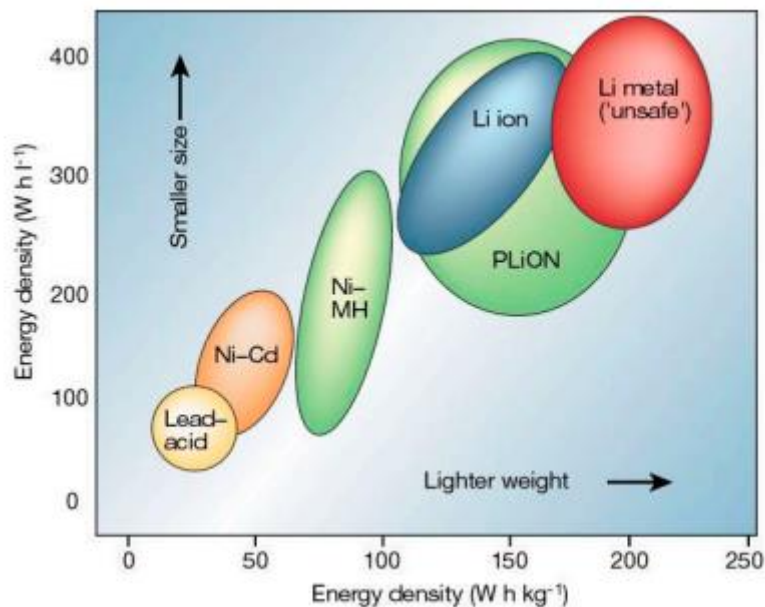


Figure 1 Energy density comparison between the most common used battery technologies in the market [6]

In this section a brief description of some of the most used battery types will be presented.

#### 1.1.1. Lead acid

Lead acid batteries are very robust and widely spread. They typically use Pb in the negative plate, PbO<sub>2</sub> in the positive plate and sulfuric acid as electrolyte. Lead acid batteries are divided into two main categories: vented and valve regulated. In the vented lead acid batteries, the electrodes are directly immersed in the electrolyte while in the valve regulated lead acid batteries, an absorbent is used to separate the electrodes from the electrolyte. Vented lead acid

batteries are common in power quality applications that typically have short lifetime range. A normal value for this type of batteries is around 1000 life cycles, which usually translates as 3 to seven years of life span. The valve regulated lead acid batteries are commonly used in uninterruptible power supply and has a life span of around 5 to 10 years. [7], [8]

The optimal operation temperature is ambient temperature, around 25°C. Some of its most common disadvantages include possible explosion danger if temperatures of -40°C are reached, degradation due to overheating, self-discharge and sulfatation which promotes cell power losses and degradation and can lead to battery failure. [8]

Figure 2 shows the basic components and chemistry of lead acid batteries.

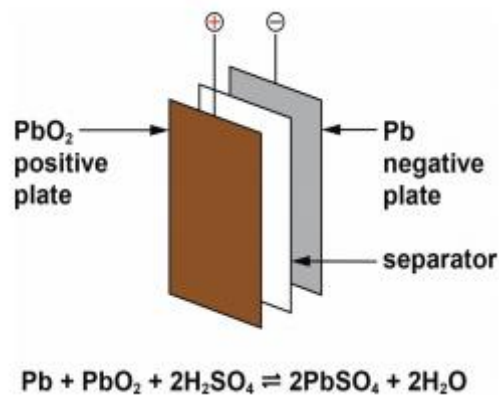


Figure 2 Lead Acid Battery components and main chemistry [7]

Lead acid batteries started to be used as early as 1870 for load leveling as well as peaking in electric plants of that moment. Since that day, this type of batteries has been used for a wide range of applications, nowadays mostly known for their use in automation. Even though they present high levels of toxicity and maintenance, coupled with low energy density and relative short cycle live, their low price, robustness and maturity keeps them as a common choice in the market.

#### 1.1.2. Nickel batteries

Nickel batteries, also known as dry cells, have always a nickel electrode, which will be positive, and a negative electrode that can be made of cadmium, iron or zinc. Nickel batteries that use cadmium in the negative electrode are the most common by far and have been properly developed and installed for storage demonstrations. The efficiency values are commonly found between 60% and 70% for NiCd batteries. They are reported to present efficiency losses and degradation due to frequency of discharge and temperature sensitivity. Life span of this type of batteries can go up to an impressive value of 3500 cycles in some cell setups with 80% usual discharge depth. [9], [10]

NiCd batteries present some important advantages: they are relatively cheap and present higher energy and power densities than lead acid batteries. They have decent life span and they are reliable. All these advantages make nickel cadmium batteries a common choice for storage applications even though they are more costly than lead acid batteries. [9], [10]

NiCd batteries present lower efficiency than the popular Lithium ion batteries and cadmium is known to be toxic, thus presenting environmental, health and safety concerns. This is especially true for the recycling of the batteries. [9], [10]

Figure 3 shows a simplified scheme and basic chemical reactions occurring in a typical Nickel Cadmium battery:

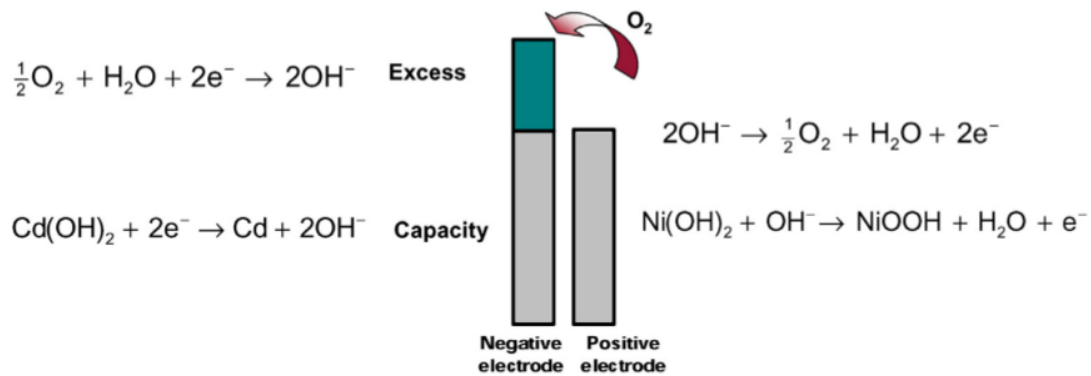


Figure 3 Simplified sealed NiCd design and chemical reactions [10]

### 1.1.3. NaS batteries

Sodium-sulfur batteries are included inside high temperature or molten salt batteries. This specific type of batteries combines some similarities of conventional batteries with thermal storage units, like its molten electrodes. Sodium-sulphur batteries use an anode made of molten sodium that can range from 300°C to 360°C and use molten sulfur as cathode. [11]

NaS primary function is energy storage for long periods of time, as they present efficiencies of up to 90% but their short response, which can be as low as 1 millisecond, also makes these batteries a good candidate for power applications. [12]

NaS batteries lifespan can be as long as 15 years and can have an estimated usage of 2500 lifecycles. However, NaS batteries are still an emerging energy storage technology with high cost as they are still in early stages of development. [11], [13]

One important caution of these batteries is the proper handling of the batteries as contact with water can cause explosions due to its high temperatures and molten state.

Figure 4 shows a basic scheme of NaS battery:

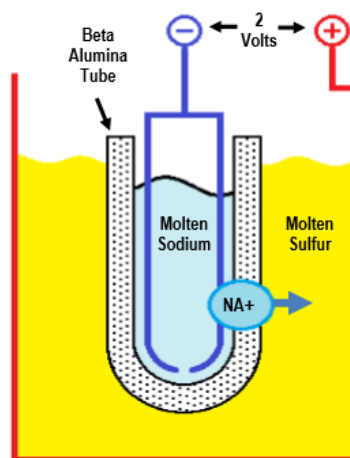


Figure 4 NaS battery scheme [12]

#### 1.1.4. Flow batteries

In flow batteries, the electrolyte is stored outside, in external tanks, and it is pumped to the electrodes where they combine to generate electricity. In this type of battery, there is a positive electrolyte, named catholyte, as well as a negative electrolyte, named anolyte. The main advantages of flow batteries are their adaptability of changing energy and power capacity to suit the wanted application as well as their relatively low energy capacity cost. Its main disadvantages are its initial cost, complexity and lack of maturity compared to other conventional batteries. [14]

The most important type of flow battery is the vanadium redox flow battery. VRB, vanadium redox flow batteries, have the same anolyte and catholyte with negatively and positively charged vanadium ions respectively, dissolved in an acid aqueous solution. They are separated with a membrane that allows ion exchange, while the current is generated in the carbon electrode. [12]

The efficiency for VBR ranges between 60-65%. Its life span is greater than most other conventional energy storage systems, as most applications often offer more than 10000 cycles. Due to their low energy density flow batteries require more volume and therefore more space than other energy storage systems. [12]

#### 1.1.5. Lithium ion batteries

A lithium ion battery consists of a negative electrode made of graphite and a positive one which is made of several metal-oxide sheets separated by a micro-porous polymer. The electrolyte is usually organic and has dissolved lithium ions in it. The oxide found in the anode is usually made of lithium and cobalt or manganese [6]. Figure 5 shows the mentioned components in a basic setup of a lithium ion battery cell:

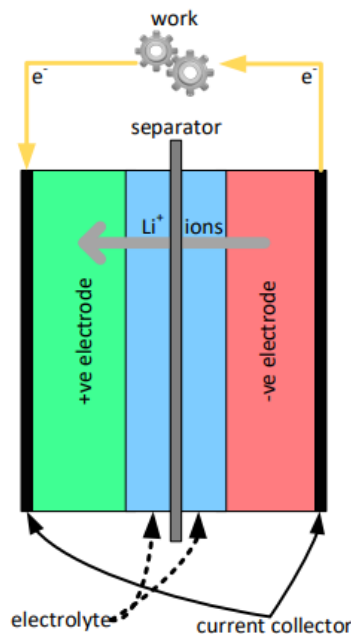


Figure 5 Basic scheme of a Lithium ion battery [6]

Lithium ion batteries have a very high energy as well as power density, which translates into higher cell voltage than most of the other batteries. One of the biggest advantages of lithium ion batteries is its high efficiency, which can reach 90% in some cells, while its life span varies between 2000 to 3000 cycles which in a typical application can last up to 10 years. [12]



Figure 6 shows a comparison of the mentioned batteries regarding some critical characteristics that determine if they are suitable for a desired application:

Battery Technologies	Applicable Capacity (MW)	Efficiency (%)	Respond Time (ms)	Life (cycle)	Investment Cost (\$/kWh)	Charge Discharge (Time)	Environmental Impact
Lead-acid	0–40	70–90	5–10	3–15(1500)	200–400	min-day sec-hour	medium
UltraBattery	0–36	–	5	3–15(3000)	200	min-day sec-hour	medium
Sodium-sulfur	0.05–34	80–90	1	10–15(2500–4500)	300–500	sec-hour sec-hour	medium
Lithium-ion	0–100	85–90	20–1000	5–15(1000–15000)	600–3800	min-day min-hour	medium
Nickel-cadmium	0–40	60–65	1–1000	10–20(2000–3500)	400–2400	min-day sec-hour	medium
Metal-air	0–0.01	50	1–1000	– (100–300)	10–60	hour-month sec-24+hour	low

Figure 6 Comparison of Battery Energy Storage Technologies [15]

As it can be seen in Figure 6 lithium ion batteries present the better capacity, efficiency and life span. Their biggest drawback is the immense investment cost that they represent, the biggest of all the mentioned battery types.

#### 1.1.6. Metal air batteries

Metal air technology, secondary batteries considered, presents the best environmental impact and the lowest investment cost, due to the high availability of its anode materials and cathode oxygen ambient air oxidant [15]. They still present low efficiency and life span due to its early stages of research and development. In this section, this battery technology will be further explained.

Metal air batteries have a metal anode and an air cathode. The metal air battery cathode uses oxygen from the air for the oxidation process, and this will lead to an important reduction of the battery weight. Metal air batteries present one other big advantage, they are cheaper than most of its competitors, especially Lithium batteries. The price is lower due to the abundance of the low-cost metals used in the anode, such as Aluminum, Magnesium or Zinc. The cathode source is oxygen from air which is also contributing to the overall low price of this type of battery. [16]

During the discharge period, oxygen from the ambient air is used as oxidant. This characteristic volume increases the energy density of the cell considerably. And even though lithium air batteries offer the best combination in the market for highest theoretical energy density and highest cell potential, 5928 Wh kg<sup>-1</sup> and 2.96 V respectively [17], Mg and Al air batteries present very similar theoretical values, as it can be seen in Figure 7.

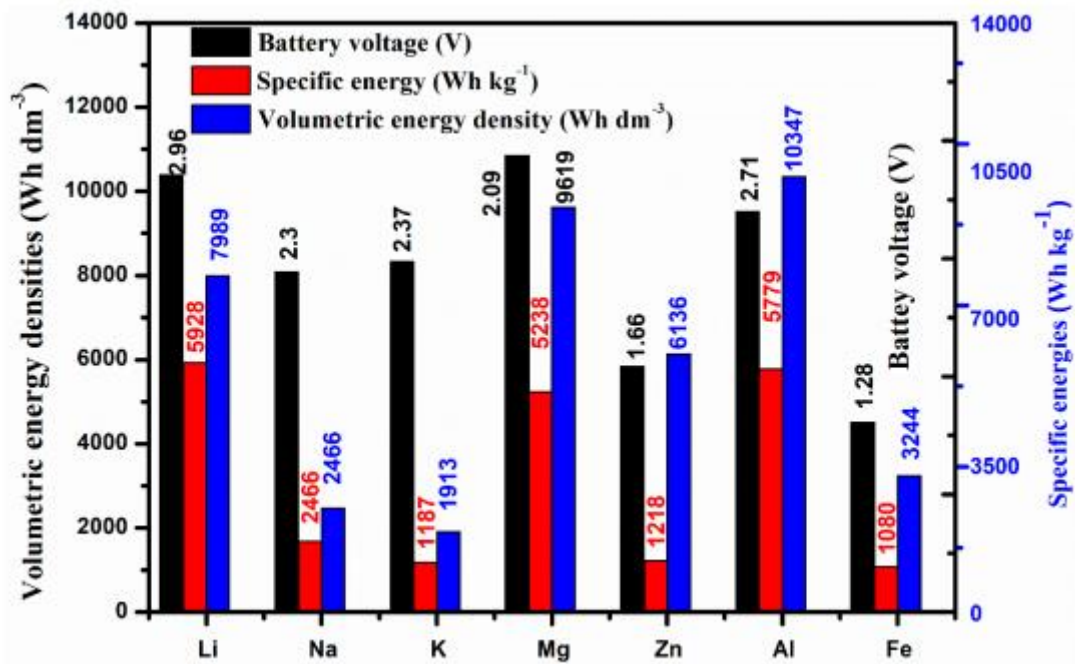


Figure 7 Comparison of Voltage, Specific Energy and Volumetric Energy Density of metal air batteries [18]

Metal air batteries have a different cathode than conventional ionic. In a typical ionic battery, the metallic ions from the anode will transfer to the electrolyte and will transfer to the cathode. In the case of metal air batteries, the metal found at the anode will transform to metallic ions while hydroxide ions will be formed in the cathode due to reduction of ambient oxygen. [19]

A way to classify metal air batteries is differentiating between aqueous and non-aqueous electrolyte systems. In an aqueous electrolyte battery, oxygen anions will be formed from the electrons that will be created when oxygen passes through the gas diffusion layer found in the cathode. The other type, the non-aqueous electrolyte batteries, metals will also release electrons, these electrons will then transform into metallic ions and dissolve into electrolytes. These processes can be better seen in Figure 8. [18]

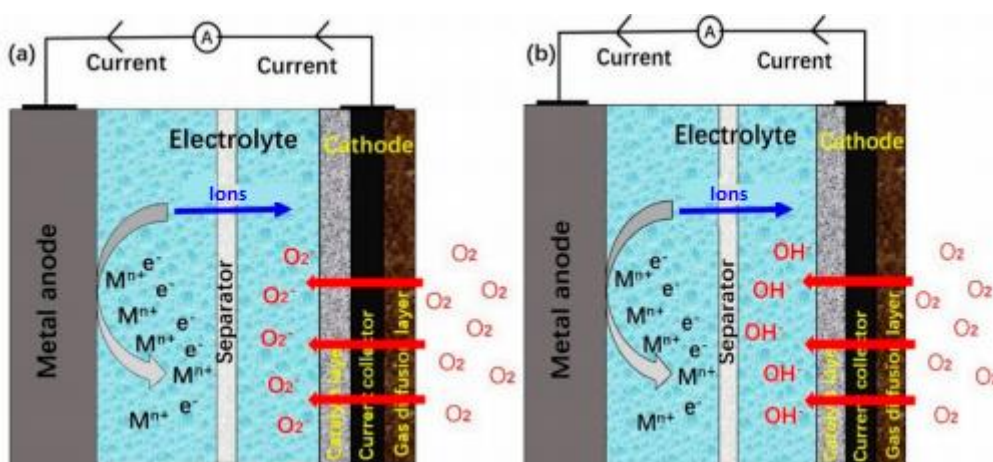
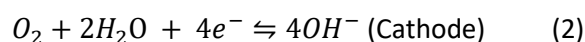
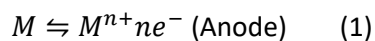


Figure 8 Basic structure and chemistry of both aqueous and non aqueous metal air batteries [18]

In metal air batteries both metal and oxygen take part in the electrochemical reactions. Reaction formulas for general metal air battery:



### Cathode

Two important chemical reactions take place in the cathode, oxygen reduction and oxygen evolution. As mentioned before, the oxygen used in these reactions is taken from the ambient. If the battery uses an aqueous electrolyte, water leakage has to be eliminated in order to preserve the cell stability.

A typical cathode found in a metal air battery is made of a current collector, a gas diffusion membrane or layer and a catalyst layer deposited over conductive carbon. If the current collector is metallic, it may use porous metals, like Nickel or Copper. On the other hand, if the current collector is not metallic, it typically uses a carbon based material like carbon (graphite, carbon cloth, etc.). [18]

Figure 9 Graphic visualization of the different layers found in a typical cathode of a metal air battery. Figure 9 shows the mentioned layers found in a typical metal air battery cathode:

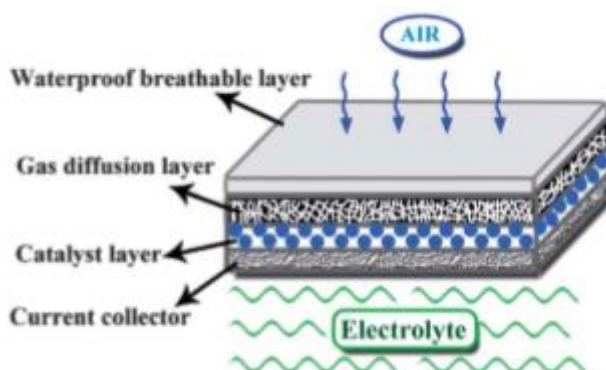


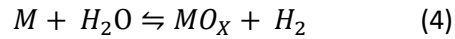
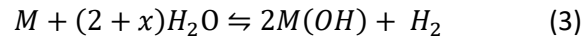
Figure 9 Graphic visualization of the different layers found in a typical cathode of a metal air battery [20]

### Anode

The anode, the negative electrode in the battery, hosts chemical activity between the metal and the electrolyte. This activity determines the discharge capacity of the cell. Due to the intense chemical activity found in the anode it is normal to see unwanted side reactions that will vary depending on the metal used, its purity, the electrolyte, the cell setup, etc. Most common side

reactions that take place in the anode of metal air batteries are corrosion, passivation and dendritic formation.

Equations 3 and 4 show the specific working principle of one of the most common corrosion reactions that takes place in the anode, the hydrogen evolution reaction:



Hydrogen evolution reaction, which takes place in the metal anode during the charge and discharge processes of the cells, is known to decrease the overall Coulombic efficiency because it consumes otherwise useful electrons found in the metal anode. Another negative side effect of hydrogen evolution is the diffusion of hydrogen inside the electrolyte which can increase the internal pressure of the battery and creates possible explosion danger.

Another unwanted side reaction is passivation. Passivated electrodes are unable to properly charge and discharge due to an insulating layer or film (called passivation layer) that blocks the exchange of ions necessary for completing the discharge process. Corrosion is also a problem as it accelerates anode dissolutions and decreases battery life. In some cases, corrosion leads to the formation of a passivation and resistive layers. This depends on the metal and electrolyte nature.

The last side reaction that will be mentioned in this section is dendritic formation and deformation. This reaction is the gradual change of the anodes metal shape, where its surface tends to become uneven and rough. This process happens when the metal ions released during discharge deposit on the anode during the charging process. After several battery cycles, the anode will accumulate dendrites and the cell will become more and more unstable.[21]

## Electrolyte

The main function of the electrolyte in metal air batteries is to transport the ions from one electrode to the other to make sure that the oxidation and reduction reactions happen. Two main types of electrolytes will be discussed in this section, the aqueous electrolyte and the non-aqueous electrolyte.

The aqueous electrolyte is the most commonly used electrolyte, these are the three main solutions found:

- Alkaline solutions: the alkaline electrolytes will have a pH above 7 but not above than 14, being the less acidic solutions for aqueous electrolytes. A lower overpotential and faster kinetic reactions make oxygen reduction more favorable and this is why alkalines are usually favored for aqueous based electrolytes in metal air batteries. The biggest drawback of these solutions is that CO<sub>2</sub> found in the ambient air will react with the electrolyte and create unwanted carbonate around the cathode. This carbonate, when found in large amounts, can block the cathode material and severely decrease the cell

efficiency. [18] Other pollutants in the air can also lead to the formation of parasitic species and poisoning of the electrodes.

- Neutral salt solution: as the name indicates, these solutions have a pH close to 7. This type of electrolytes is usually used in aluminum air battery, due to the lower corrosion rate that they generate compared to the alkaline electrolytes.
- Acidic solutions: these solutions will have a pH lower than 7. Acidic electrolytes are demonstrated to accelerate H<sup>+</sup> production which translates into a reduced battery efficiency. This is why they are not commonly used in actual metal air cell setups. [18]

There are two main types of non-aqueous electrolytes:

- Solid-state electrolyte: This type of electrolytes differs from the aqueous electrolytes mainly in ion conduction and wettability. In a solid-state electrolyte, the three phased interface reaction can be restrained due to the low wetting property of the electrolyte, and this can facilitate the transportation of OH<sup>-</sup> compared to an aqueous system. Alkaline gel electrolytes have been developed (especially for primary lithium air batteries) in order to reduce this phenomenon. This gel has low molecular weight and low acidity. [18]
- Ionic liquid electrolyte: This type of electrolytes has few applications due to the formation of carbonates and the lack of information and research done regarding the oxygen reaction in an ionic liquid. The main agent in these electrolytes are large organic cations with both organic and inorganic anions and alkali ions inside a solvent. [18]
- Polymeric (organic) electrolytes: Polymeric electrolytes have the potential to reduce several drawbacks such as hydrogen evolution, dendrite formation, unwanted extra water evaporation in the electrolyte, and carbonation [22]. They also typically provide higher and wider temperature range, which can be very useful for specific applications. On the other hand, it is important to decide which composition to use in order to avoid problems like volatility, flammability and toxicity. Those are the main reasons why traditionally the metal-air battery's electrolyte has been an aqueous solution that enables ion's transportation between anode and cathode. [22]

### **Strategies to improve rechargeability**

These following strategies aim to improve both Oxygen Reduction Reaction (ORR) and Oxygen Evolution Reaction (OER) in order to achieve better rechargeability:

- Bifunctional air catalysts: oxygen catalyst that can fulfil efficiently both ORR and OER. One example of it is metal oxide, as it is linked with the ability of the cations to embrace different valency states [23]. A thin layer of this material on a carbon substrate treated with hot air has proved to be a great catalyst with bifunctional activity that resembles the catalyst properties of precious metals. Bifunctional electrodes are still in early stages of development and its life cycle is still too short as degradation limits harshly its number of cycles. In the case of metal oxides, it is known to have tendency to get oxidized to MnO<sub>4</sub><sup>-</sup> as well unwanted corrosion in the carbon substrate found in the catalyst. [23]

- 3 electrode configuration: A cell design that utilizes two air electrodes to charge and discharge. The third electrode is then placed between these two air electrodes and when it discharges it connects to the reductive electrode while changing to the evolution reaction electrode for charging. Life span of the cell is greatly improved because this procedure avoids the contact of ORR catalysts to the oxidative potential and the OER catalyst to the reductive one. The major drawback is the decrease in both energy and power density due to the increased cell volume. [23]

## 1.2. Mg Air batteries - State of the art

One of the more promising materials to use in the anode of metal air batteries is magnesium. Mg-air batteries have very high theoretical energy density of around 6800 Wh/kg. In terms of specific capacity Mg-air batteries have around 2200 Ah/kg and a theoretical cell voltage of 3.1 V, even though actual cell voltages will be approximately half of that value [24]. These numbers are similar or even superior to that of a Lithium ion battery [20]. A global use of Mg-air battery, like it is found with Li-ion batteries, is not possible now due to several factors. These 4 are the most important ones:

- Narrow operating voltage of around 1.2 V, due to high polarizability of the electrodes [20]
- Low faradaic efficiency due to unwanted parasitic reactions such as hydrogen evolution or formation of thick corrosion layers
- Sluggish oxygen reduction reaction kinetics at the cathode
- Poor recharge ability due to uneven Mg deposition and formation of corrosion layers

Figure 10 shows the basic structure and working principle of a Mg air battery:

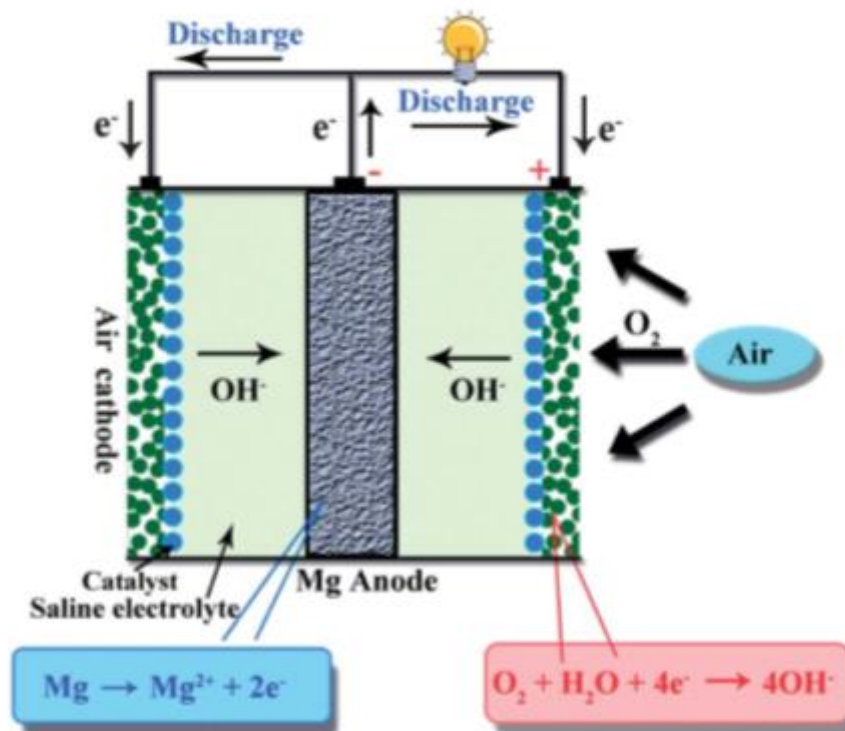
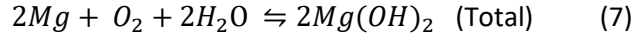
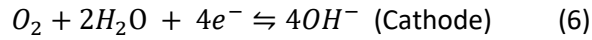
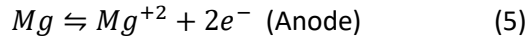


Figure 10 Basic structure and working principle of a Mg air battery [20]

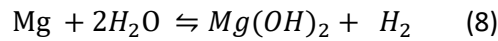
Mg air batteries have a very similar behavior to the conventional primary batteries. The biggest difference is that the cathode will be made of a conductive carbon layer where reduction of oxygen from external air takes place. Since the oxygen reactant is not stored in the battery, there is a reduction of the volume and mass needed and this increases the specific capacity and energy density of the battery (this is a common feature with the other metal air batteries). During discharging of a metal–air electrochemical cell, the reduction reaction involves the reduction of oxygen from ambient air at the cathode, as it can be seen in the right side reaction of Figure 10, and in the meantime the metal anode is oxidized, as it can be observed in the left side reaction of Figure 10.

The reactions that can be found in a typical magnesium air battery are shown in Equations 5, 6 and 7:



The electrode that is more of interest for this project is the anode and the reactions that occur around it. During the discharge process, the magnesium found in the anode is dissolved to produce ions. The standard potential in the anode's reaction is -2.37 V and can produce up to 2.2 A h g<sup>-1</sup>. [20]

Corrosion is a side reaction that greatly influences the overall performance of the cell and thereby must be taken into consideration. The overall corrosion reaction equation of the magnesium air battery cell is a combination of the anode, cathode and product reactions and can be seen in Equation 8:



### Magnesium alloys

Figure 11 shows the most commonly used magnesium alloy anode materials for Mg air batteries:

Type		Main constituents	Morphology	Properties	Ref.
Simple Mg	Commercial Mg	Mg	—	High corrosion rate, large negative difference effect	1
	Nano/mesoscale Mg	Mg	Nanospheres Nanoplates Nanorods Urchin-like	Better corrosion resistance and high current density as well as higher rate discharge ability than commercial Mg	19
Mg-alloy	AZ31, AZ61, AZ91 <sup>a</sup>	Mg/Al/Zn	—	Better corrosion resistance, better strength and tarnish resistance and higher working voltage than commercial Mg	12 and 18
	AM50, AM60, MA8M06 <sup>b</sup>	Mg/Al/Mn	—	Better corrosion resistance, smaller crystalline grains and higher working voltage than commercial Mg	20
	Mg-Li alloys	Mg/Li	—	Better corrosion resistance, higher energy density and higher working voltage than commercial Mg	18 and 21

<sup>a</sup> AZ31 (96 wt% Mg, 3 wt% Al and 1 wt% Zn), AZ61 (93 wt% Mg, 6 wt% Al and 1 wt% Zn), AZ91 (90 wt% Mg, 9 wt% Al and 1 wt% Zn). <sup>b</sup> AM50 (~94 wt% Mg, 5 wt% Al, 0.6 wt% Mn), AM60 (~93 wt% Mg, 6 wt% Al, 0.6 wt% Mn), MA8M06 (~97 wt% Mg, 1.3 wt% Mn, 0.12 wt% Zn, 0.12 wt% Al, 0.2 wt% Fe).

Figure 11 Different types of magnesium alloys anode materials for Mg air batteries [20]

It is a common practice to introduce alloying metal elements, like aluminum, zinc, manganese, tin and indium in order to decrease corrosion rate produced in the Mg anode. In this thesis, and due to availability and academic reasons, AZ31 is used, although using different electrolyte solutions and inhibitors, researchers have found that AZ61 alloy to be superior to AZ31 regarding cell voltage and hydrogen evolution rate. More alloying elements have also been tested, such as heavy metals like cesium, lead and gallium, and also light metals like aluminum, lithium and calcium [25]. Some of these alloys, such as Mg-14Li-1Al-0.1Ce have presented higher operating voltage, anode utilization efficiency and lower self-discharge than AZ31 alloy and even pure magnesium. Other studies show that adding Ca helps the alloy Mg-6Al-0.3Mn-2Ca get a higher capacity as well as efficiency, especially with low operating current. A recent study found the



optimal composition of Al, Sn and Mn in a magnesium alloy anode using orthogonal design and showed that the proportions of composition Mg– 6Al–1Sn–0.4Mn give the higher discharge potential as well as corrosion resistance. [25]

### Electrolyte

Figure 12 shows the corrosion (rest) potential of pure magnesium in different aqueous solutions in a 3.5 wt.% for each electrolyte:

Electrolyte	$E_r$ (V vs. NHE)
NaCl	-1.72
Na <sub>2</sub> SO <sub>4</sub>	-1.75
HCl	-1.68
HNO <sub>3</sub>	-1.49
NaOH	-1.47
NH <sub>3</sub>	-1.43

Figure 12 Rest potential of magnesium anode when immersed in different aqueous electrolytes [20]

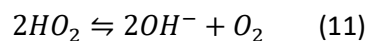
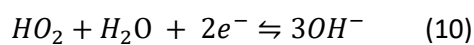
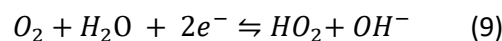
It is observed that magnesium anodes have higher corrosion resistance in alkaline electrolytes than in acidic or neutral ones. This is due to the formation of Mg(OH)<sub>2</sub> layer on the anode surface. In theory, this phenomenon protects the anode from corrosion, but if the layer is too thick it also eliminates the necessary reactions between anode and electrolyte. That is why neutral solutions are commonly preferred in magnesium air cells. [25]

Apart from the pH of the solution, it is known for the anions to play an important role in the corrosion process. Cl<sup>-</sup> and SO<sub>4</sub><sup>2-</sup> have proved to increase the corrosion rate while NO<sub>x</sub> ions are likely to be less aggressive and thus mitigate the corrosion rate. [25]

Another factor that can influence the corrosion is the amount of salt found in the electrolyte solution. Low concentrations of salt are found to be less corrosive with the anode. [20]

### Air cathode

When a neutral solution is used in the cell, O<sub>2</sub> is transformed to OH at the interface of the gas–solid–liquid ternary phases located in the air electrode. Complex chemical reactions occur when the Oxygen Reduction Reaction happens in the three-phase interface [20]. Typically, the reactions involved in the Oxygen Reduction Reaction in a neutral electrolyte are Equations 6, 9, 10 and 11:



The standard electrode potential of ORR, which can be seen in Equation 6 is 0.44 V. However, a high overpotential and polarization are typically seen in the ORR, which ultimately leads to a bad cell performance due to the sluggish kinetics of the reaction. In order to achieve lower overpotential, efficient catalysts are needed as explained in the previous section. The direct four electron process seen in Equation 6 is the most efficient, so having a four-electron catalytic ability is a desirable quality in an optimal catalyst material. [20]

Magnesium batteries provide very high energy and they have several advantages over other batteries, including lithium based ones. Magnesium is much more common and less expensive as more mineral can be extracted from the mines. It is also safer, as it reduces the risks of explosion and fire and it is much less prone than lithium to suffer failures in its internal structure. Several studies show how unstable lithium can be, especially when in contact with water or aqueous solutions and, comparatively Mg is less reactive.

However, these types of batteries are still not commercially competitive until they can store and discharge large amounts of energy. But magnesium air batteries have been studied for several decades now and are pin pointed as a solution for various applications. [26]

The first noticeable magnesium battery that allowed a reversible electrochemical dissolution appeared in the early 1990s. Different electrolytes were proposed for these secondary magnesium air batteries, which could be recharged, but all of them had very poor results. This meant that no commercial rechargeable prototype could be assembled yet.

This first secondary magnesium battery that successfully demonstrate rechargeability used an electrolyte made of  $\text{Mg}(\text{BPh}_2\text{Bu}_2)_2$ . However, it was found that this compound has a very low stability against electrochemical oxidation, and this was the main cause of the low operating voltage of this first cell, which operated under 2 V. Since that first demonstration many different compounds, electrolytes, additives and inhibitors have been tested to improve the Mg air cell voltage as well as the amount of cycles that the cell can do before it has to renew electrodes/electrolyte. Substitution of the boron with aluminum or hydrogen is also being tested to help enhance its oxidative stability. [26] Figure 13 illustrates the effect of this enhancement methods and how they compare with a typical lithium ion battery.

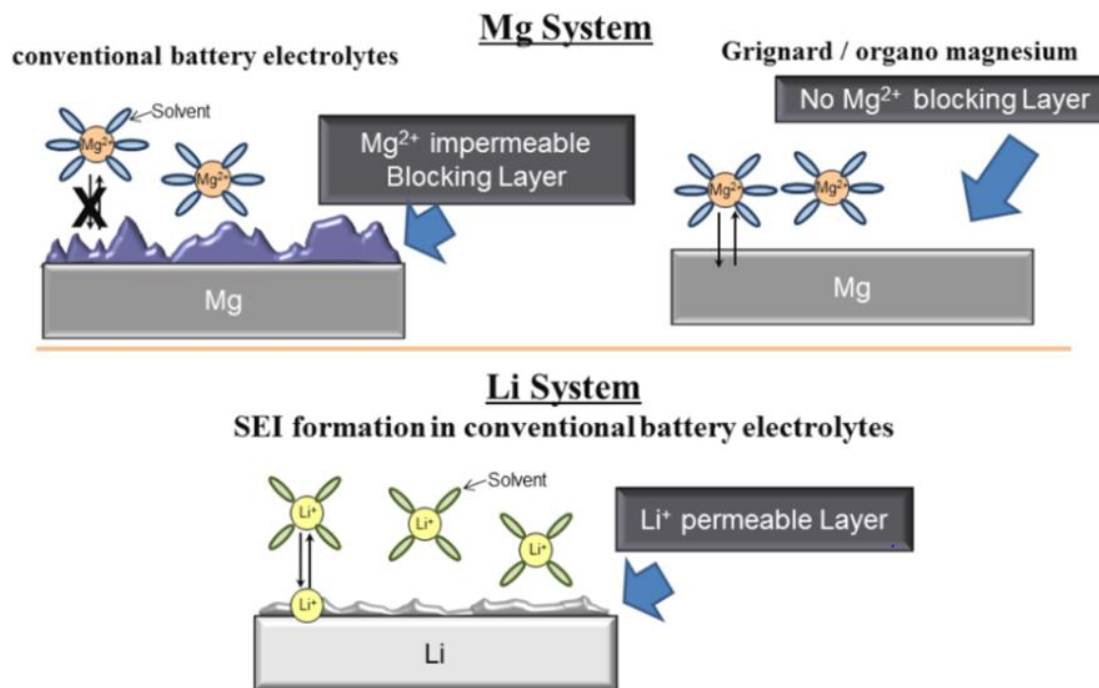


Figure 13 Mg system vs. Li system [26]

The scientific community has been motivated to overcome the mentioned problems and research efforts recently started switching from typical organohalo aluminates to organoborate based electrolytes, and many more additives and reagents become of interest. [26]

### 1.3. Future

It is wide-spread and well known that secondary magnesium air batteries have huge potential for both industry and society. CNN wrote an article stating that in 15 years, half of the world car production will be electric. Coupled with smartphones and laptops, the market is there. The problem is that the technical challenges together with cost effective high-energy density cathode material, stable anodes and appropriate electrolytes that will not produce unwanted and sluggish reactions slowed down the progress of these type of batteries. One of the biggest reported problems has been the formation of an unwanted, non-conductive layer onto the anode of the cell, which has a negative impact on the battery recharge and lifetime. Back in 2016 Honda's Saitama ITC, announced that they had finally overcome these underwhelming problems and have already produced a commercially viable Mg air secondary (rechargeable) battery using a cathode containing vanadium.

Different scientific groups, universities and private research centers have been investigating the use of magnesium in metal air batteries as a replacement for lithium, which is the most competitive secondary battery in the market at the moment.

Magnesium has two main advantages over lithium. The first one is that Mg is much more abundant than lithium and this makes it much cheaper too. The second one is that Mg has higher energy density. It has a density over volume that can be up to 50% higher of lithium and besides this important factor, Mg does not need to be intercalated in a compound layer, making Mg air batteries reach a relative volumetric density until 5 times higher than their lithium ion counterparts.

As mentioned before, electric vehicles will gain more and more popularity in our society. Magnesium air batteries can play a crucial role in this field, as they have the theoretical capability of extending the range of the electric cars if they also mentioned problems and drawbacks can be overcome. Magnesium has higher energy density than lithium, so if two batteries of the same size are made with these two metals, Mg air batteries will be able to pack more energy in the same space.

It is unquestionable that rechargeable lithium ion batteries have been dominating the battery market since their commercialization in the decade of the 90s. They are the undisputed kings of electric vehicles and portable electronic devices main energy sources. Lithium can be very unstable though, especially if in contact with  $H_2O$ . Lithium is also more expensive than magnesium and its availability raised serious concerns among users and manufacturers. That is why the industry is switching its interest to other alternative metals that can fulfill this role, like magnesium. In that sense, both Mg air and Mg ion batteries are finding a lot of interest. [24]

An article published in 2018 by Ruigang Zhang and his colleagues reported very interesting results about a hybrid battery using magnesium and sodium. [27] Even though these batteries are not metal air batteries, the corrosion principle in the magnesium anode is very similar to the ones described and studied in this thesis and thus also interesting for the project.

A magnesium sodium hybrid cell utilizes the magnesium which is deposited in the anode without any dendritic formation combined with the rapid  $Na^+$  intercalation in the cathode to create the possibility to charge and discharge the cell several times, obtaining the desired secondary magnesium battery [27]. By utilizing this specific design principle, a Mg- $NaCrO_2$  hybrid cell was constructed using a magnesium anode, a cathode consisting of  $NaCrO_2$  and a mixture of  $PhMgCl-AlCl_3$  with Mg-APC and  $NaCB_{11}H_{12}$  as dual-salt electrolyte [27]. The Mg- $NaCrO_2$  hybrid battery was tested during 50 cycles and was able to deliver 2.3 V and an energy density of 183 Wh  $kg^{-1}$ . Using solid  $MgCl_2$ , the researchers found that the amount of electrolyte could be reduced without affecting the electrochemical properties and performance of the cell [27]. The paper also presented and proposed a hypothetical  $MgCl_2$ - $NaCrO_2$  hybrid battery with an approximated voltage of over 2 V and the energy density of 215 Wh  $kg^{-1}$ . [27]

This article is in the early stages of developing this technology and further research is needed to see if the prototype could be commercially available [27].

Magnesium air batteries still present major issues especially related to the anode corrosion. In primary batteries, the coulombic efficiency is greatly reduced due to Mg reactivity, high corrosion rate (even in alkaline solutions) and presence of unwanted precipitation of insoluble magnesium hydroxide in the anode [25]. In secondary batteries, the main issue that makes this technology still in its very early stages of development is the difficulty of transforming magnesium oxides back to useful magnesium. [25]

This thesis objectives aim to help and broaden the research on corrosion inhibition of the magnesium anode in Mg air batteries, as explained in the following section.

## 2. Corrosion inhibitors for the Mg anodes

The main objective of this thesis is to control the corrosion process in the anode of magnesium air batteries. As mentioned in the previous sections, magnesium has a lot of energy density potential and advantages over other anode materials used for the purpose, but its biggest drawback is how fast corrosion occurs and the occurrence of unwanted reactions that happen at the surface of the anode when in contact with the electrolyte.

For this reason, the experimental part of this project is going to be divided between experiments done in blank electrolyte and experiments done with an added corrosion inhibitor. First, the corrosion process in the anode will be studied when it is immersed in a blank electrolyte using four different electrochemical techniques that will be thoroughly discussed and explained in the methodology part: Open Circuit Voltage, Electrochemical Impedance Spectroscopy, Galvanostatic Discharge and Potentiodynamic Polarization

The results obtained using the blank electrolyte will be compared with results obtained using the same electrolyte plus a corrosion inhibitor. The four same electrochemical techniques used in the first part will be repeated in order to obtain a proper comparison of the results.

Even though the most used electrolyte for magnesium air batteries is NaCl, it was decided that in this project NaNO<sub>3</sub> is going to be used instead.

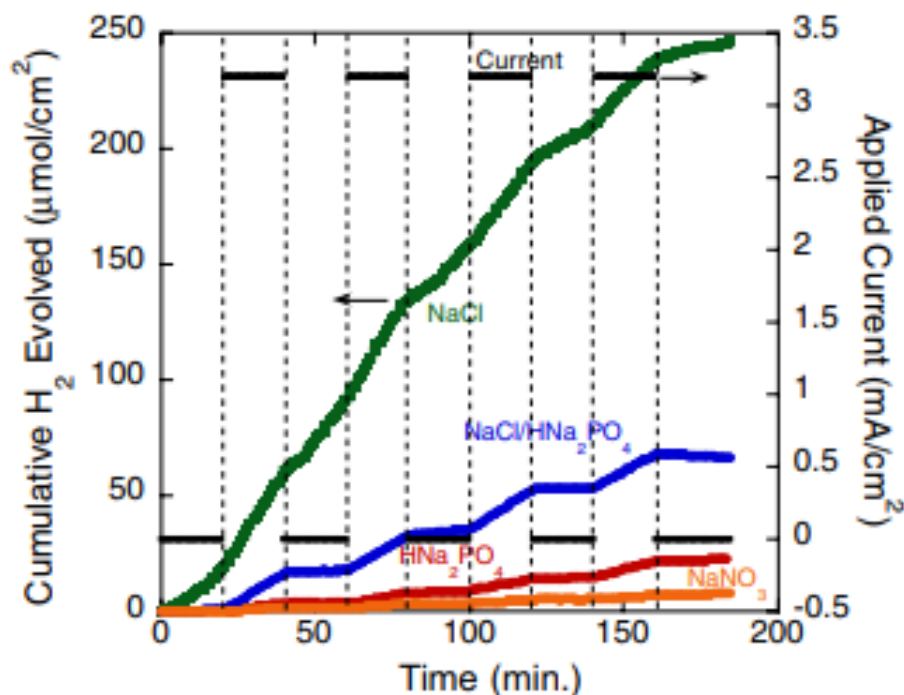


Figure 14 Different electrolyte solutions comparison regarding cumulative H<sub>2</sub> evolution [28].

There are some points that influenced the decision of choosing NaNO<sub>3</sub> over the more conventional approach base NaCl:

- NaNO<sub>3</sub> presents the least hydrogen evolution of all the different electrolytes as it can be observed in Figure 14. H<sub>2</sub> evolution is directly linked to the corrosion process and can be considered a measure of the corrosion rate [28].

- The same report also stated that  $\text{NaNO}_3$  presents the highest faradaic efficiency, when different cell setups were tested and compared between these 4 main electrolytes used in Mg air batteries [28].
- It also provided the lowest OCP (open circuit potential). This is due that the results were negative, so the lowest OCP would imply a biggest different of potential and thus a better and more powerful Mg battery.
- Final and not least,  $\text{NaNO}_3$  offers the biggest room for improvement. NaCl has been thoroughly studied, and as this is an academic project,  $\text{NaNO}_3$  was more appealing as it has been less studied and experimented with, opening the way for novel discoveries and improvements, especially when coupled with specific inhibitors that are not also heavily used nowadays.

The decision of which inhibitor to use required a more intense literature search. There are many scientific publications and reports that show how different inhibitors affect the corrosion in magnesium, but there is no data of how they affect a Mg air battery that uses  $\text{NaNO}_3$  as electrolyte. After some literature search and critical analysis of that, it was decided to use sodium phosphate, known for its corrosion inhibiting properties in magnesium [29]. A brief section at the end of the chapter shows the current research on the inhibiting effects of sodium phosphate.

It is important to mention that it was not intended to completely eliminate the corrosion found in the anode, as it is necessary for the proper functioning of the battery. The main purpose was to obtain a controlled corrosion rate, which would allow to obtain the highest possible outcome parameters of the cell and to open the possibility of recharge. This is a very challenging objective and so far, researchers still did not succeed on finding the balance between corrosion and corrosion inhibition on the Mg battery anode. This is a critical step to move further the Mg air technology.

### **Magnesium inhibitor corrosion research**

There is very scarce or no literature that presents magnesium air batteries using  $\text{NaNO}_3$  as electrolyte and tests different inhibitor. In this section, some of the inhibitors that have been studied using standard NaCl as electrolyte will be presented.

In 2018, Daniel Höche and his colleagues presented an article that studied how seven different substances would affect corrosion inside a magnesium air cell using NaCl as electrolyte. The seven substances were: catechol-3, 5-disulfonic acid disodium salt (Tiron), ethylenediaminetetraacetic acid dipotassium salt (K2-EDTA), and sodium salts of salicylate, glycolate, oxalate, nitrilotriacetate (NTA) and dodecylbenzenesulfonate (DBS). They are shown and compared in Figure 15 regarding hydrogen evolution. It was seen how Tiron, which is an iron complexing agent, would have a positive impact in the performance of primary magnesium cells. [30]

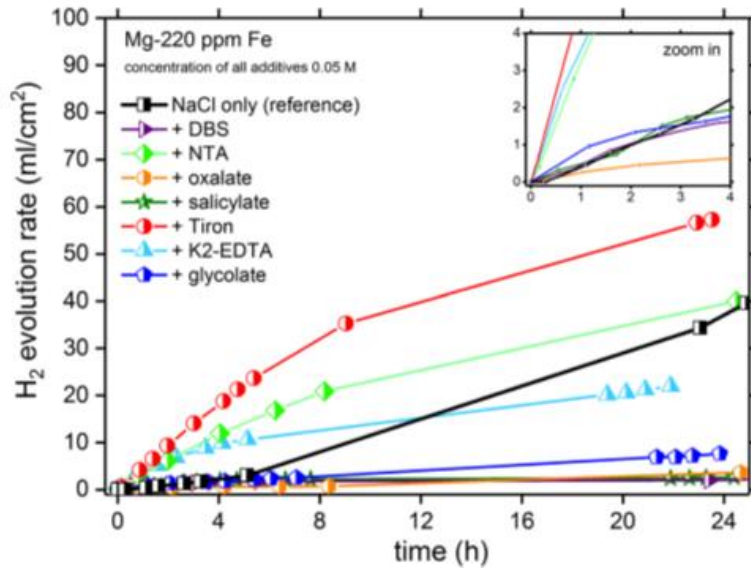


Figure 15 Comparison of different inhibitor corrosion substances to improve performance of primary Mg cells [30]

In 2016, Yan-Chun Zhao and his colleagues published an article proving how corrosion inhibitor  $\text{Li}_2\text{CrO}_4$  greatly improved the performance of Mg air batteries. In their experiment it was seen how adding 0.1 wt % of this inhibitor in a solution of NaCl would enormously reduce the corrosion current density in their samples, which used AZ31 Mg alloys as the ones used in this thesis. The anode efficiency of the final cell was increased by an impressive 28.4 %. [31]

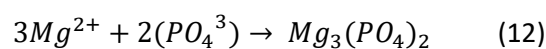
In 2016, the Egyptian Petroleum Research Institute presented an article on how Decyl Glucose increased the Mg-air overall battery performance. According to the paper, a maximum inhibition efficiency of 94% was achieved using Decyl Glucose in a NaCl electrolyte and the anode offered higher operating voltage, discharge curves and anodic efficiency than the blank electrolyte. [32]

Many researchers and scientists studying corrosion science have been testing different anions and inhibitors to mitigate corrosion in Mg anodes. The effects and properties of organic and inorganic inhibitors such as decyl glucoside, lithium chromate, water soluble graphene, sodium silicate, sodium alginate, sodium phosphate and sodium dodecylbenzenesulfonate have been explored by researchers.

#### Sodium Phosphate as a selected corrosion inhibitor

Recent results show that discharge potential of the cell and the anode utilization of Mg air battery greatly increase with the addition of sodium phosphate. In the experiment, alloy AZ91 was used in the anode with an aqueous electrolyte of 3.5 wt% NaCl and an addition of 0.5 g/L sodium phosphate [29].

The results of the experiment showed that the discharge potential increased from 1.1 V to 1.15 V and the anode utilization increased from 44.1% to 49.1%. The corrosion inhibition efficiency reached 95.2% and the self corrosion had a tendency to decrease [29]. Equation 12 shows the reaction of sodium phosphate and magnesium ions inside the cell:



### 3. Methodology

#### 3.1. Sample preparation

The sample preparation will be equal for all the tests in order to achieve maximum reliability. First of all, a plate (4x3 cm, 2 mm of thickness) of alloy Mg AZ31 is polished using four different sandpapers in a polishing machine. SiC papers of four different grit sizes were used: 280, 360, 600 and 1200 of the European FEPA or P-Grading.

The composition of the magnesium alloy AZ31 is 97% Magnesium, 2.5-3.5% Aluminum, 0.6-1.4% Zinc, 0.2% Manganese, 0.1% Silicon, 0.05% Copper, 0.04% Calcium, 0.005% Iron and 0.005% Nickel. All the percentages are calculated in weight. [33]

An exposed area of 3.65 cm<sup>2</sup> was defined thanks to glued acrylic tubes onto the metal surface. In order to make sure that the setup is completely sealed, the immersions in electrolyte will be held 24 hours after.

The blank electrolyte consisted of an aqueous solution with 0.5 M of NaNO<sub>3</sub>, and approximately 10mL of solution were used in each sample.

In Figure 16 the electrochemical set up used is shown. Apart from the magnesium plate, that is the working electrode, the acrylic tube and the electrolyte mentioned in this section, the reference and counter electrodes can also be seen. These parts of the equipment will be discussed later in this chapter.

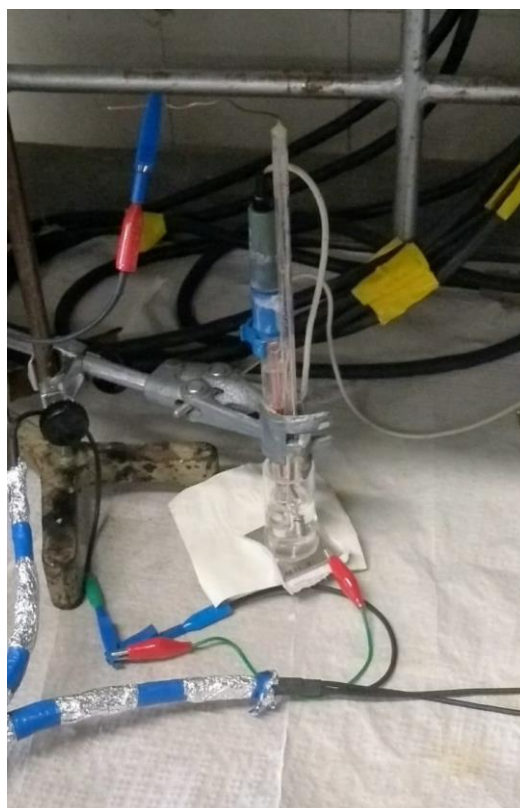


*Figure 16 Testing of a sample in the Reference Gamry 600+*



## 3.2. Equipment

### Potentiostats

Potentiostats are capable of measuring and controlling the potential of the cell, detecting changes in its resistance, and varying the intensity of current administered to the system according to these variations, so that the potential difference will remain constant. If the resistance increases, the intensity of the current must be decreased to keep the voltage constant, and if the resistance decreases, the potentiostat should increase the intensity of the current. It is an application of Ohm's law. It is a basic equipment in corrosion and electrochemical studies

The potentiostat requires the use of an electrochemical cell and the respective electrodes, namely a working electrode (the Mg alloy), a counter electrode (Platinum) and a reference electrode (Saturated Calomel Electrode - SCE). These last 2 electrodes should not interfere with the chemical process that is being studied at the working electrode. Voltages or currents are always imposed to the working electrode.

Important characteristics to be taken into account in a potentiostat are the following: range of electrical potential that can be measured and that is capable of applying, precision in the electrical potentials, range of electrical current that the instrument can measure and apply and number of working electrodes that the instrument can handle.

This instrument manages to maintain a constant potential difference in the working electrodes, taking as reference the voltage in the reference electrode and correcting the variations by controlling the current in the auxiliary electrode.

Figure 17 shows the potentiostat that was used in most of the experiments that were carried out. It is the model Gamry Reference 600+.



Figure 17 Gamry Reference 600+

## Working Electrode

The Working Electrode is the electrode where the potential is controlled and where the current is measured. The Working Electrode serves as a surface where the electrochemical reactions of interest take place.

In corrosion tests, the Working Electrode is a sample of the corroding metal. The Working Electrode can be a bare metal or a coated metal. In this specific work it was a sample of Mg that simulates the anode.

## Reference Electrode

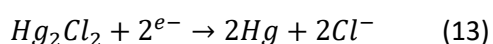
The main purpose of the reference electrode is to measure the potential in the working electrode. In the setup used in this project, the reference electrode is the Saturated Calomel Electrode. No current is flowing through the reference electrode, so it should have constant electrochemical potential. The most wide-spread and commercialized reference electrodes are the saturated calomel electrode, more commonly known as SCE, and the silver/silver chloride electrodes. It is worth to note that the hydrogen electrode is the reference to the existing electrode potentials.

The standard hydrogen electrode, which is reversible, is made of a platinum electrode immersed in an acidic solution containing 1 M of protons and hydrogen gas at a pressure of 100 kPa. The absolute potential is 4.44 V at ambient temperature but it is typically set to zero as reference. [34]

The major drawback of the normal hydrogen electrode is that its preparation is cumbersome, and also its handling, since a gas (H<sub>2</sub>) is needed. Therefore, in practice it is replaced by others that have proven to be good reference electrodes because they are capable of maintaining a very constant potential.

The SCE is constructed by depositing in the bottom of a liquid mercury container; on it Hg<sub>2</sub>Cl<sub>2</sub> (or a paste of this salt and Hg); and above all a solution of KCl of known concentration. The device includes a platinum wire that is inserted until it contacts the liquid Hg. The purpose of KCl is to keep a property called ionic strength constant; that way the potential measures are stabilized. It is possible to select between using a solution saturated in KCl or unsaturated. In the first case, the electrode is called saturated calomelanos.

The potential of this electrode depends on the concentration of KCl and the temperature. It is easier to prepare the saturated Calomel electrode than the unsaturated one, since it is enough to add KCl to water until it no longer dissolves. Its drawback is that its potential varies with temperature more than that of the unsaturated. The reduction reaction that occurs in a calomel electrode is shown in Equation 13:



The potential of the saturated calomel electrode measured against the hydrogen standard is 0.2444 V at ambient temperature. It does not function to find determinations at over 60 °C because Hg<sub>2</sub>Cl<sub>2</sub> decomposes.

## Counter Electrode

The counter electrode, sometimes denominated auxiliary electrode, is a conductor that allows the current flow through the cell setup.

The Counter Electrode in lab cells is generally an inert conductor like platinum or graphite. In field probes, it might be another piece of the Working Electrode material. The current that flows into the solution via the Working Electrode leaves the solution via the Counter Electrode.

The electrodes are immersed in an electrolyte (an electrically conductive solution). The collection of the electrodes, the solution, and the container holding the solution are referred to as electrochemical cell.

### 3.3. Techniques

#### 3.3.1. Open Circuit Potential

The open circuit potential (also known the equilibrium potential, the rest potential, or the corrosion potential) is the potential at which no net current is flowing, so experiments based on the measurement of the open circuit potential are considered potentiometric experiments. Such measurements are very basic and simple, they have many important applications, which will be discussed briefly in this section.

The basic equation of potentiometric concentration measurements is the Nernst equation, which relates the concentration of electroactive species at the electrode surface to the potential at that electrode (E). Equation 14 shows the Nernst equation.

#### Nernst equation

$$E = E_o + \frac{0.059 \text{ V}}{z} \log_{10} \frac{a_{\text{Ox}}}{a_{\text{Red}}} \quad (14)$$

Where:

- $E_o$  is the formal redox potential of the electron transfer reaction.
- $a$  is the chemical activity for the selected species,  $a_{\text{Red}}$  is related to the reduced form and  $a_{\text{Ox}}$  is related to the oxidized form
- $z$  is the total number of electrons that enter the cell

The potential  $E$  is measured between two electrodes: the working electrode and the reference electrode (the auxiliary electrode is disconnected for potentiometric measurements). The working electrode is selected such that its potential is sensitive to the concentration of the analyte in solution (e.g., a glass membrane electrode for the measurement of pH), and the reference electrode (e.g., the saturated calomel or the silver/silver chloride electrode) provides a stable reference potential for the measurement of the potential of the indicator electrode.

In battery studies important measurements include the open circuit potential of a battery, and the equilibrium (corrosion) potential of a corroding system.

The evolution of these potentials provides important information on the working electrode behavior and are very simple to carry out.

### 3.3.2. Electrochemical Impedance Spectroscopy

Electrochemical impedance spectroscopy (EIS) is a powerful technique that utilizes a small amplitude, alternating current (AC) signal to probe the impedance characteristics of a cell. The AC signal is scanned over a wide range of frequencies to generate an impedance spectrum for the electrochemical cell under test. EIS differs from direct current (DC) techniques since it allows the study of capacitive, inductive, and diffusion processes taking place in the electrochemical cell. EIS has far reaching applications including coatings, batteries, fuel cells, photovoltaics, sensors, and biochemistry.

EIS is most commonly run in 3 electrode mode. In this configuration there is a working electrode (the Mg sample), counter electrode (graphite and platinum are commonly utilized), and an independent reference electrode--Saturated Calomel Electrodes (SCE) or Silver/Silver Chloride (Ag/AgCl) which are the most common.

The results obtained from running EIS are shown in different plots, being the most common ones Bode and Nyquist plots.

As a brief description of these two different ways to show the EIS results, the Bode plots show the frequency response of the studied system. There are two Bode plots that are typically shown together, the first one for magnitude and the second one for phase angle. The Nyquist plot, on the other hand, combines both magnitude and phase into one plot in the complex plane. It is drawn by plotting the complex magnitude, for example  $m(i\omega)$ , for all frequencies  $\omega$ . The plot is then a curve in the plane parametrized by all frequencies ( $\omega$ ).

An examples of Nyquist plots and magnitude Bode plots are displayed in Figure 18:

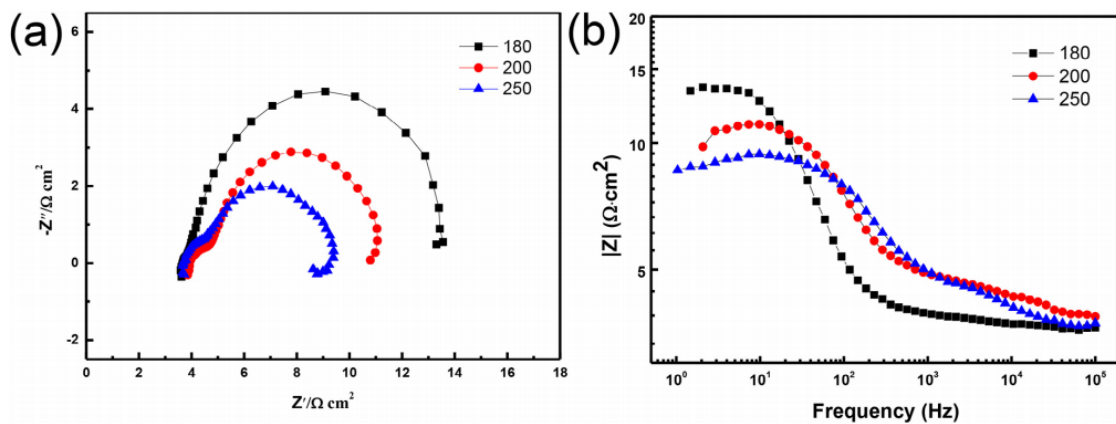


Figure 18 EIS results of pure magnesium samples in 3.5 wt% of NaCl solution. (a) Nyquist plots and (b) Bode plots. 3 samples of pure magnesium (99.95 wt.%) ingots are extruded at the temperatures of 180 °C, 200 °C, and 250 °C, respectively. [35].

### 3.3.3. Potentiodynamic Polarization

Potentiodynamic Polarization a quick testing technique commonly used in material corrosion studies to gain corrosion rate data. For this method the material is polarized, typically on the order of  $\pm 10\text{mV}$ , relative to its Open Circuit (OC) potential—the potential measured when no [net] current is flowing. As the potential of the material (working electrode) is changed, a current will be induced to flow between the working and counter electrodes, and the material's resistance to polarization can be found by taking the slope of the potential versus current curve. This resistance can then be used to find the corrosion rate of the material using the Stern-Geary equation, shown in Equation 12 and 13:

$$Rp = \frac{B}{i_{corr}} \quad (12)$$

$$B = \frac{b_a * b_c}{2.3(b_a + b_c)} \quad (13)$$

Where

- $i_{corr}$  is the corrosion current
- B is the proportionality constant
- $b_a$  and  $b_c$  are the Tafel slopes

#### 3.3.4. Galvanostatic Discharge

The study of the variation of the response of the current over time under galvanostatic control is called galvanostatic discharge. With this technique the working electrode is subjected to an instantaneous potential change from the initial potential to another for a certain time.

The working electrode is introduced into the electrolyte and subjected to an initial potential, corresponding to the electric double layer potential formed between the electrode and dissolution. When the potential jump occurs, the double layer has to adjust to a new potential, so that, when collecting the variation of the current density over time, a large initial peak is obtained.

## 4. Results and discussion

### 4.1. Potentiodynamic Polarization

Potentiodynamic Polarization results are shown first in the experimental part as it provides useful information. Both anodic and cathodic obtained Tafel curves can be obtained. In this case the technique was used to assess the best inhibitor concentration to be used in the rest of the experiments.

The first results were obtained in blank  $\text{NaNO}_3$  electrolyte in order to have a benchmark to compare the inhibitor results when sodium phosphate is added. Three different inhibitor concentrations will be tried in the second part: 0.05 M, 0.01 M and 0.005 M.

#### 4.1.1. Blank electrolyte results

The following graphs show both the anodic and cathodic curves together. The voltage range for both sides is 0.3 V from the OCP values determined before for each sample. This means that for the anodic curve will move, from the OCP value into the positive direction 0.3 V, while the cathodic one will move 0.3 V into the negative range. The scan rate was 0.15 mV/s in each case.

It is important to mention that the anodic and cathodic curves were obtained in different samples and the results are plotted together. This is the right procedure to avoid interferences of the cathodic curve in the anodic response.

In these plots the voltage in the y axis is plotted against the logarithm of the intensity over the area. This is very useful as it eliminates the total area factor when comparing different samples.

Figure 19 show the anodic and cathodic polarization resistance curves 24 hours after immersion.

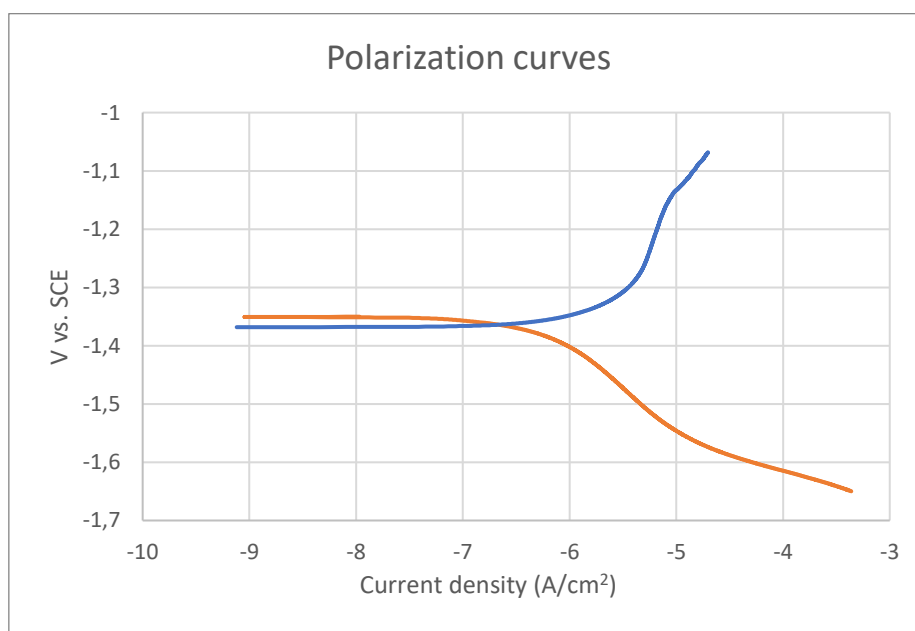


Figure 19 Anodic and Cathodic Polarization resistance curves using blank electrolyte.

One of the first results that can be observed from the plot is the two curves do not match perfectly, because the two curves are not obtained in the same sample. Theoretically the OCP should be the same, but small impurities, surface imperfection or even environmental factors can have an influence on the result. Nevertheless, the OCP results obtained are similar to the ones obtained in the OCP values using only blank electrolyte and they are also similar to each other (the lines almost coincide) indicating good reproducibility.

Both anodic curves reveal a regular increase of the current density with potential and both curves are under charge transfer kinetic control because the currents increase regularly with potential. No relevant diffusional effects could be observed in the cathodic curve. It is worth to mention that extraction of quantitative parameters from polarization curves obtained on Mg samples is not an accurate procedure due to the specificities of the corrosion mechanism and intense gas release. Therefore, only comparative discussion will be made in this section.

Literature on the usage of  $\text{NaNO}_3$  as electrolyte for magnesium air batteries show that the results obtained using blank  $\text{NaNO}_3$  electrolyte are in good agreement with previous work [28], and that the OCP of the Mg electrode is higher than when NaCl is used. The values found in various articles are more or less -1.4 V for  $\text{NaNO}_3$  and -1.6 V for NaCl [28]. This is negative for the battery as having a higher potential in the anode using this electrolyte will result in a lower discharge voltage. As seen in previous sections,  $\text{NaNO}_3$  electrolyte is known to provide reduced  $\text{H}_2$  evolution compared to NaCl, so the negative increase found in the OCP using Potentiodynamic polarization suggests that a different corrosion reaction is occurring. Nitrate to nitrite corrosion is considered to be the principal cause of this secondary corrosion, as experiments on  $\text{NO}_2^-$  titration show an increase of  $\text{NO}_2^-$  when  $\text{NaNO}_3$  is used [28].

#### 4.1.2. Results with inhibitor

In this section d.c. polarization was used to study the inhibitor addition effect and also to study the effect of inhibitor concentration to determinate if this would have a relevant effect on the mechanism and corrosion potential. Thus, three concentrations of inhibitor: 0.05 M, 0.01 M or 0.005 M sodium phosphate are tested.

##### 0.05 M Sodium phosphate

For this inhibitor concentration the corrosion potential was slightly more negative than -1.3 V and the current density increased with potential, as expected, revealing a charge transfer control.

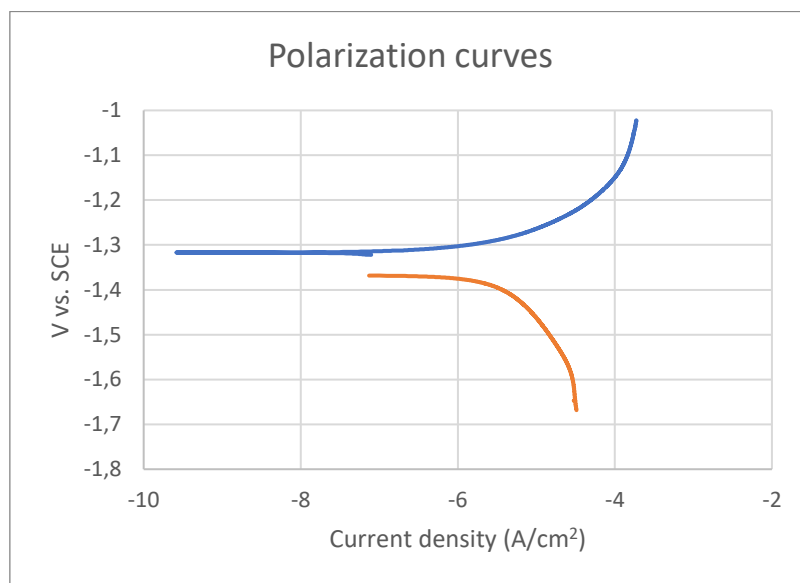


Figure 20 Anodic and cathodic curves in the same graph using 0.05 M sodium phosphate.

As it can be observed in Figure 20 the OCP has remained almost unaltered. In fact, it has even slightly increased compared to Figure 19 , which was tested using blank  $\text{NaNO}_3$  electrolyte. This is not a positive result as a less negative potential in the anode will result in a lower discharge battery voltage.



### 0.01 M Sodium phosphate

Considering the intense gas release observed, at early stages in the sample exposed to 0.05 M, it was decided to decrease the inhibitor concentration, according to the concentration values observed in the literature [29], [31], [32], [36]. The curve depicted in the figure below shows that there is a decrease of the corrosion potential towards more negative values indicating a strong cathodic polarization effect.

No significant differences could be observed on the anodic and cathodic current densities and also the mechanism seems to remain the same.

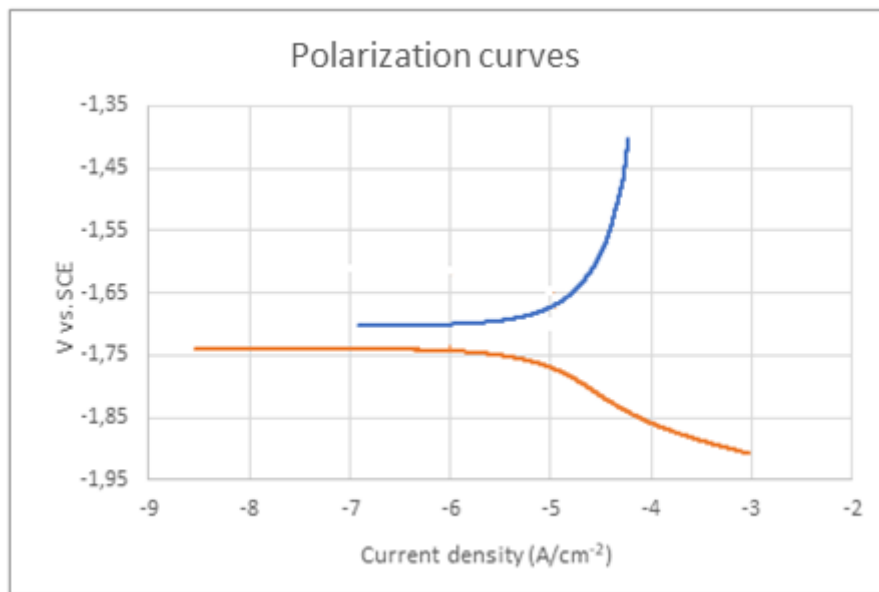


Figure 21 Anodic and cathodic curves in the same graph using 0.01 M sodium phosphate.

The first noticeable impression seen in Figure 21 is that the OCP has greatly decreased, and thus increasing the overall potential of the cell, as it is shown as a negative value. This is very positive for the aiming of this project and will be further discussed.

### 0.005 M Sodium phosphate

This specific inhibitor concentration was the third and last concentration of sodium phosphate tested. It was decided to use this low concentration to evaluate if further cathodic polarization effects would be observed. The OCP remains very similar to the OCP obtained using 0.01 M, and as commented before this is positive for the battery. No relevant shifts on the corrosion potential are noticed in Figure 22 and the current densities remain in the same range. Interestingly the anodic curve reveals a faster increase in the region near the corrosion potential compared to the previous ones. This may account for easier Mg dissolution in this case.

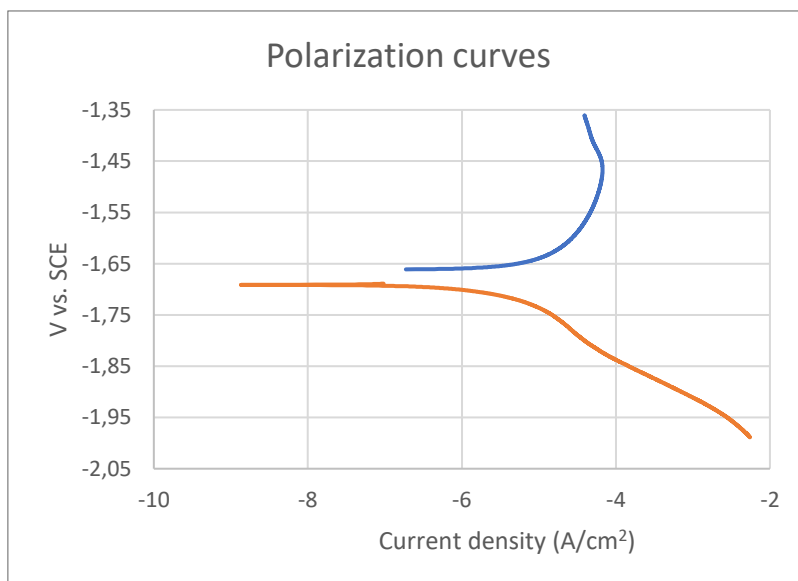


Figure 22 Anodic and cathodic curves in the same graph using 0.005 M sodium phosphate.

#### 4.1.3. Comparison and discussion of the results

In Figure 23, the anodic curve of all the three concentrations: 0.01 M, 0.05 M and 0.005 M are shown. The anodic curve of the sample that used only blank electrolyte is also shown for better visualization and comparison of the samples.

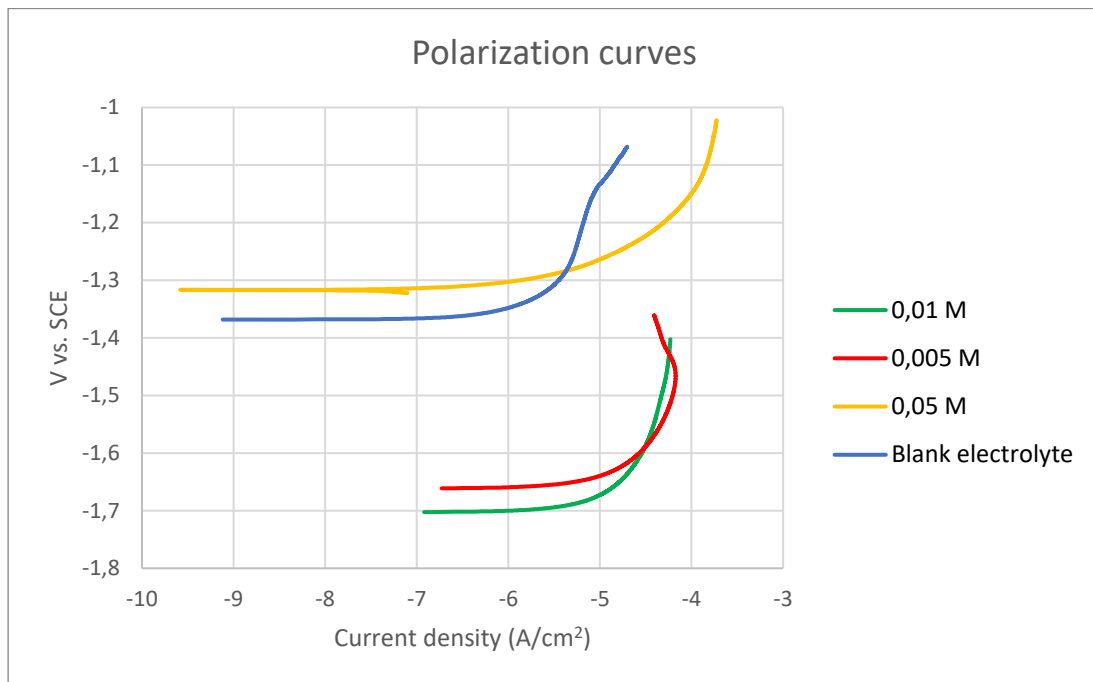


Figure 23 All anodic curves plotted together

Clearly, lower concentrations induce an important decrease of the OCP benchmark value that is obtained prior to the polarization of the samples, towards more cathodic values, evidencing that in this case the cathodic reaction is strongly polarized. The anodic current densities are very similar and one order of magnitude lower than the ones in the presence of 0.05M, which is closer to the behavior in the blank solution. The most important conclusion is that decreased inhibitor concentrations cause an important cathodic polarization effect and increase the anodic current density. This may also account for easier and faster Mg dissolution. Contrarily the highest concentration places the curve closer to that of Mg in the blank electrolyte, with identical corrosion potential and identical corrosion rate.

It is known for sodium phosphate to decrease OCP in the magnesium anode when added as corrosion inhibitor in the electrolyte, as it prevents the erosion of  $\text{Cl}^-$  [29]. Experiments show that it can decrease around 0.1 V when an AZ91 Mg alloy is immersed in a solution of NaCl with sodium phosphate. In this experiment, using AZ31 Mg alloy and  $\text{NaNO}_3$  solution, it decreases almost 0.4 V.

## 4.2. Open Circuit Potential

The main purpose of the Open Circuit Potential was to observe the anode behavior during the first 24 h of immersion and to determine at which moment the sample was already stable so it would also be easier to conduct other experimental techniques that required stabilized samples where corrosion had already created a passivated layer on top of the magnesium anode. Furthermore, a comparison of these parameters between blank electrolyte and adding inhibitor will be conducted.

### 4.2.1. Blank electrolyte results

The open circuit potential evolution is an indicator of the Mg alloy response in the electrolyte. Typically, an increase reflects formation of a more protective layer whereas sudden fluctuations may account for corrosion activity.

Figure 24 shows the behavior of the open circuit voltage of AZ31 in 0.5M NaNO<sub>3</sub> in an aqueous solution.

The results show all the points measured in the first 24 hours of the sample's immersion. In order to appreciate more the behavior in the beginning of the immersion, where more points are concentrated, there are graphs for different intervals of this experiment in the OCP section of the Annex 1.

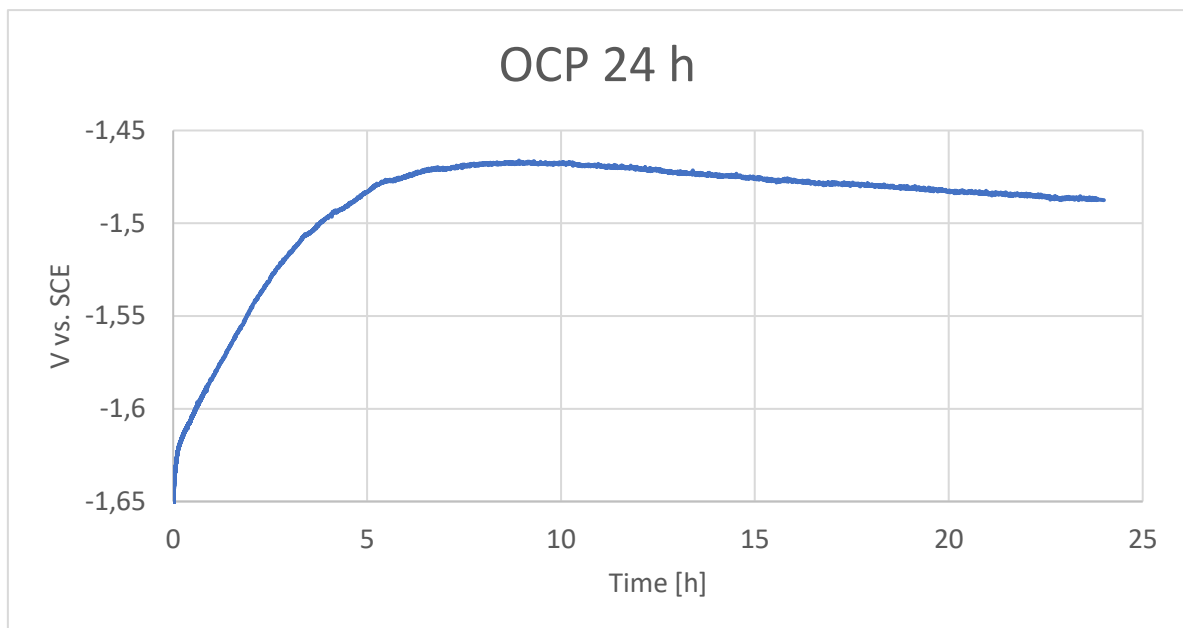


Figure 24 Open Circuit Potential using blank electrolyte during the first 24 h of immersion

The behavior of AZ31 immersed in NaNO<sub>3</sub> is similar as if it was immersed in NaCl solution, but it seems to stabilize a bit later [37]. This means that it takes more time to create the passivation layer or it makes a thicker one.

On the other hand, when compared to the samples that are immersed in a KOH solution, the ones using either NaNO<sub>3</sub> or NaCl present a much smoother curve, without the characteristic falls that appear in the OCP tests that run Mg alloys with KOH electrolyte solutions [38].

Figure 25 shows the OCP points during the 25<sup>th</sup> hour after making the immersion. As it can be observed, the total open circuit potential only decreases 0.0006V making it a negligible change. This is interesting to analyze, as it shows that the sample has reached stabilization, in fact most of the articles stop calculating OCP after 30 min to one hour as it is assumed that the sample is stable enough [29], [31], [37]. The overall increase reflects the formation of a stable surface layer, resulting from Mg oxidation and further precipitation of Mg hydroxides (these hydroxides come from the oxygen reduction).

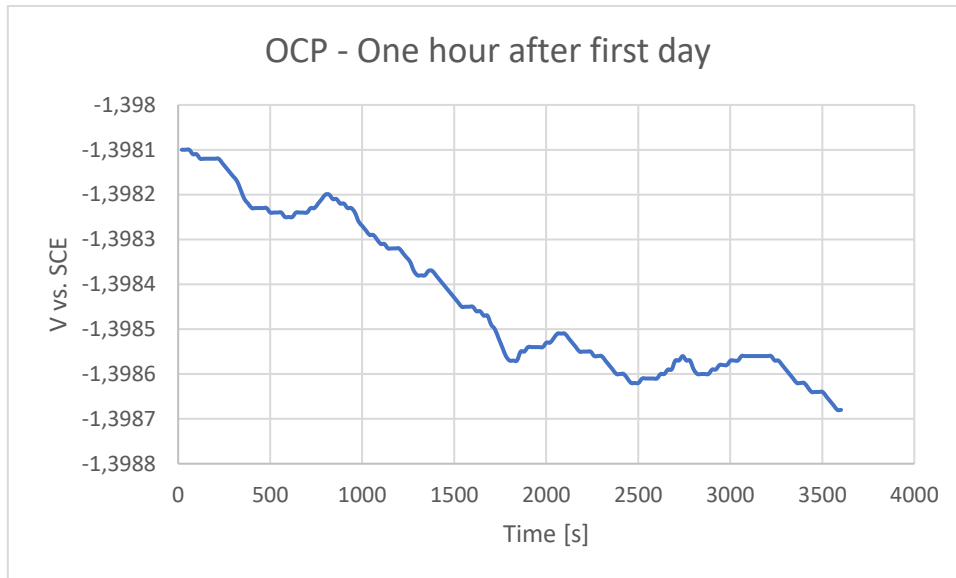


Figure 25 OCP on the 25<sup>th</sup> hour after immersion

#### 4.2.2. Results with inhibitor

Once the behavior of the magnesium when immersed in blank electrolyte ( $\text{NaNO}_3$ ) was plotted, it was important to understand how it was affected when sodium phosphate was added to the electrolyte. In this case, 0.01 M of sodium phosphate concentration was used in the electrolyte, as it showed during the potentiodynamic polarization and chronoamperometry tests that it seems the most ideal of the three different concentrations of inhibitor substance that were tested during this experimental part.

Since OCP values are obtained without applying any extra current or voltage to the sample, their results only offer a general view of the behavior of the final cell setup. This is why this experiment was left for the last one and only one inhibitor concentration was used, the one that looked more promising as mentioned in the previous paragraph.

Figure 26 shows the behavior of the first 24 h of immersion:

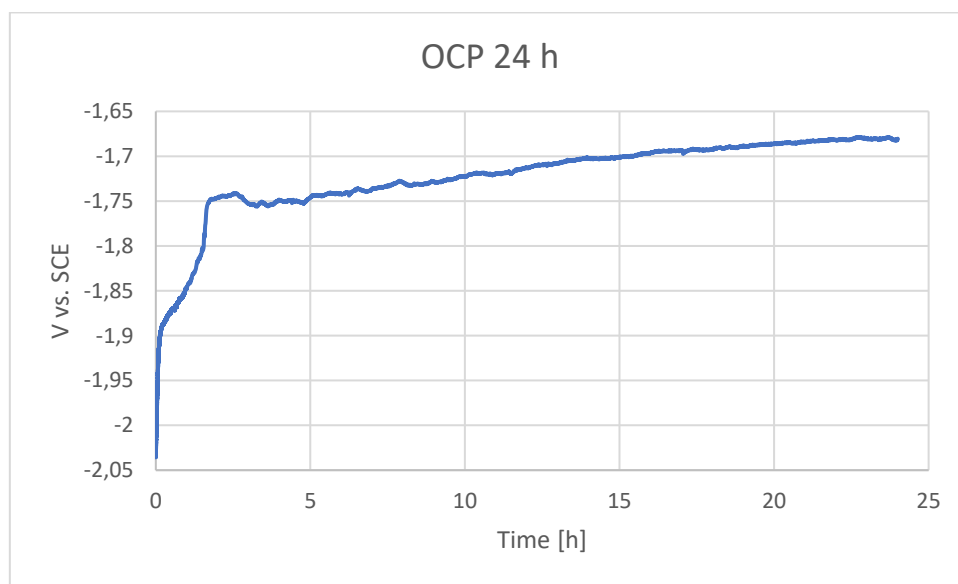


Figure 26 24 h OCP with inhibitor

The most important feature is a drop of the corrosion potential at early stages of immersion that was more negative than in the absence of inhibitor. Over time, potential increased, similarly to the what was observed for Mg in the blank solution. As it can be observed, the tendency line could also be identified as logarithmic, but it is definitely more irregular than the one obtained using only blank electrolyte.

It is very interesting to observe that the OCP obtained when an inhibitor was used is more negative than the one obtained using only electrolyte, in both the first moment of immersion and after 24 h, when the sample in both cases is stabilized already. This pinpoints that the presence of inhibitor affects the cathodic reaction, i.e the oxygen reduction. This follows the trends shown when Mg alloys are immersed in a NaCl solution with sodium phosphate [29], although as mentioned in the Potentiodynamic Polarization section, the decrease when this inhibitor is combined with  $\text{NaNO}_3$  is even larger than the ones using NaCl [29].

#### 4.2.3. Comparison and discussion of the results

The first and most important parameter to compare is the potential values of the two curves. When not using any inhibitor the first OCP of -1.65 V is obtained when the sample is immersed, and a value of -1.49 V when the sample is stable after 24 h. On the other hand, when using an inhibitor, an initial value of -2.05 V is obtained and a final value of -1.69 when the sample is stabilized, 24 h after. One thing that can be extracted from these values is that the difference between the initial points is double the difference obtained in the final points. Just after sample immersion, there is a difference of 0.4 V between using inhibitor and not using inhibitor, but after 24 h this difference is only 0.2 V. This is mainly due to the initial behavior of the sample with inhibitor, it can be observed a very intense increase in voltage, almost perpendicular to the x axis.

It is also very interesting to see how the shape of the curve changes between both conditions. When not using an inhibitor, the line is smoother, with its values having less oscillations, there are no small peaks in between and the line follows a well-defined logarithmic trend.

The inhibitor was likely to accelerate Mg dissolution at early stage, leading to the formation of a compact corrosion layer that appeared right after immersion in the sample exposed to inhibitor. This phenomenon was observed constantly during the experimental part and could explain this initial voltage drop and the previously mentioned less smooth behavior of the curve. In order to show what could be visually seen during the experiment, the samples were taken to the microscope in order to compare the two samples.

Both of these factors can be explained more easily when looking at the optical comparison of the two samples (Figure 27):

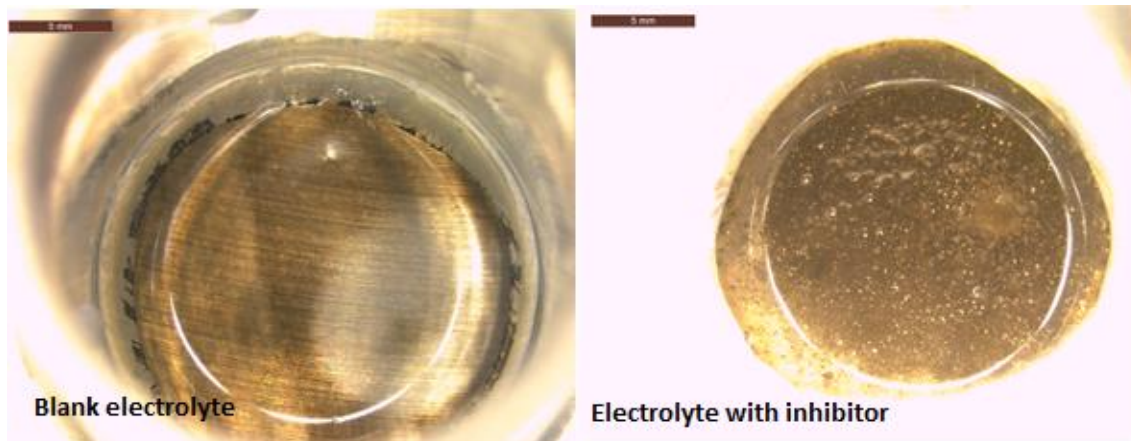


*Figure 27 Optical comparison between the two samples*

It can be seen that a thick surface layer is formed when the inhibitor is used. Over time this layer forms a protective cape that will difficult contact between the original electrode surface and the electrolyte. Thus, it can be concluded that the presence of the corrosion inhibitor decreases the open circuit potential to more negative values promoting the formation of a layer of magnesium compounds, likely  $Mg(OH)_2$  that forms a stable, but probably porous barrier.

To further understand the phenomenon, the following experiments were performed.

### 4.3. Electrochemical Impedance Spectroscopy

EIS is a powerful technique because it allows to understand the mechanism of the processes occurring at the surface and at extracting important information such as the protectiveness of the layers formed at the surface and how this change over time. Moreover, fitting of spectra can allow determining quantitative parameters.

#### 4.3.1. Blank electrolyte results

The experiments were conducted during a time span of 7 days. During these 7 days, four measurements were made in order to see how EIS was evolving with time. Results are shown in Figure 28:

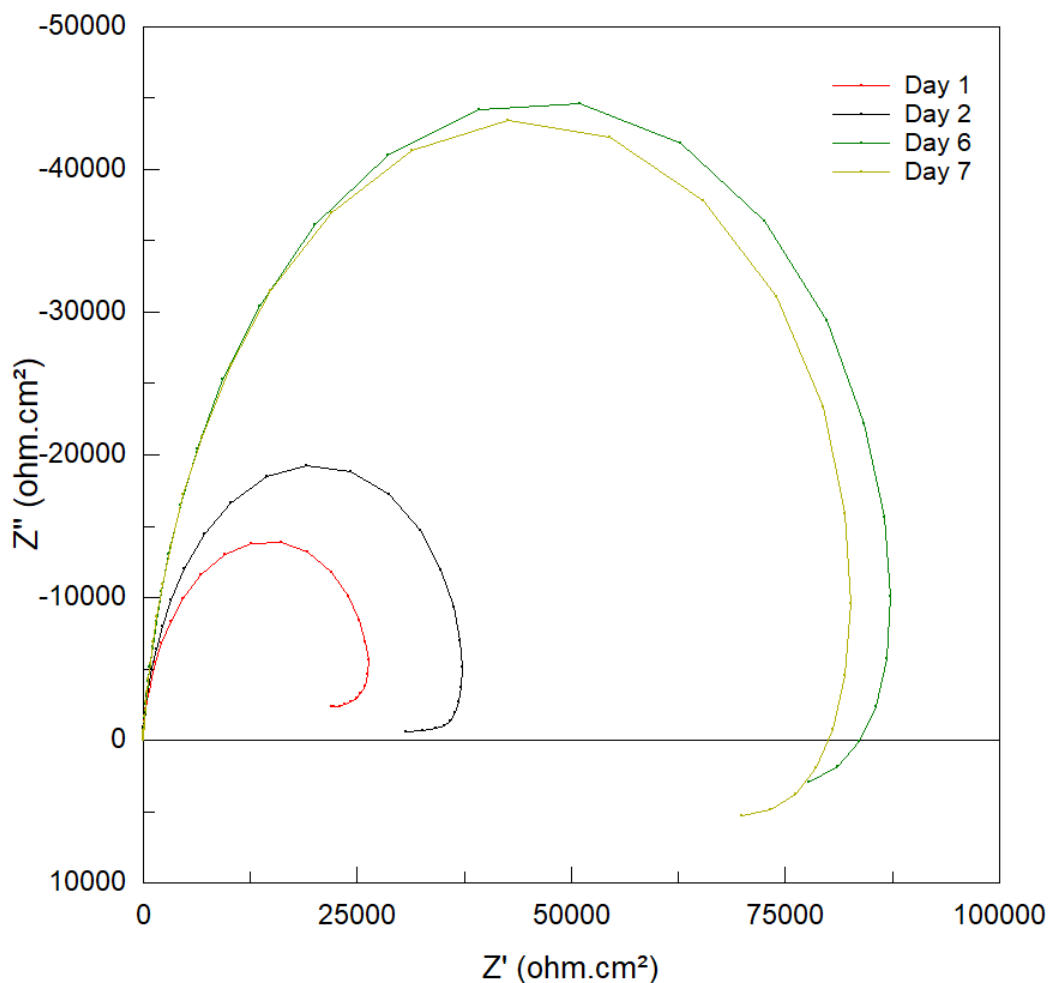


Figure 28 Impedance Nyquist plot using blank electrolyte

These results clearly show an increase of the capacitive impedance loop over time and the formation, in the low frequency range of an inductive loop. The impedance changes were notorious during the first days but become attenuated from 6 to 7 days, reaching a stabler condition. The presence of the inductive loop is related to corrosion activity and formation of intermediate Mg ions ( $Mg^+$ ) that are released from the surface.

It is also helpful to analyse the Bode plots. These plots present the same data as the Nyquist plot, but in this case the impedance modulus or phase angle will be plotted against the



frequency, evidencing how both the capacitive and resistive regions change, the phase angle also gives information about time constants, which means the processes that are ongoing. As seen in Figure 29, the capacitive region remains almost unchanged (the phase angle remains the same for all samples) and the main differences are the increase of the low frequency impedance for approximately 4 times over the immersion time.

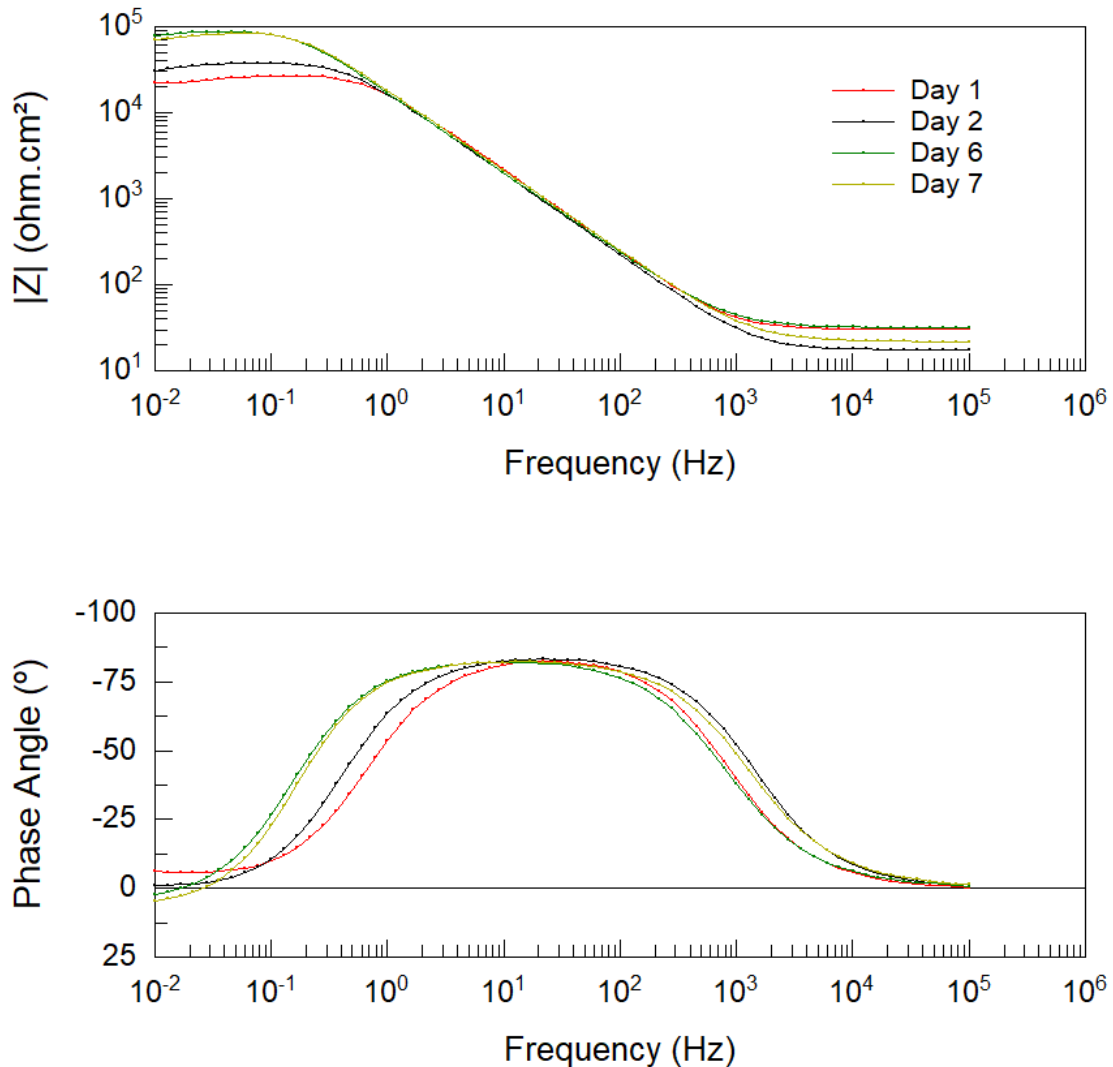


Figure 29 Impedance Bode plot using blank electrolyte

The values of the low frequency impedance are an indicator of the corrosion activity of the working electrode and here it can be observed that this activity decreased over time by a factor of 4. This is due to accumulation of protective corrosion products that decrease the electrode area. This, in case of a Mg anode will contribute to decrease the active area of the electrode. These stable corrosion products will have to be reverted in case the material is used as electrode and the battery recharged.

The impedance results obtained in the Nyquist plot and the Bode magnitude plot are much higher, around two orders of magnitude, compared to the research done with AZ31 anodes immersed in NaCl that are done right after immersion [28], [30]. Impedance greatly increases

with time, especially in Mg alloys compared, for example, to Al alloys [39]. The values obtained correspond to the values found with stabilized samples in other reports [39].

#### 4.3.2. Results with inhibitor

In this second part of the electrochemical impedance spectra (EIS), the same experiment will be held, using the same equipment setup and time span. The only aspect that will differ from the original experiment is that 0.01 M Sodium Phosphate will be added to the previously used electrolyte. EIS measurement were taken after days 1, 2, 6 and 7 days of immersion.

Figure 30 is the Nyquist plot, where the real and imaginary part of the impedance are plotted together:

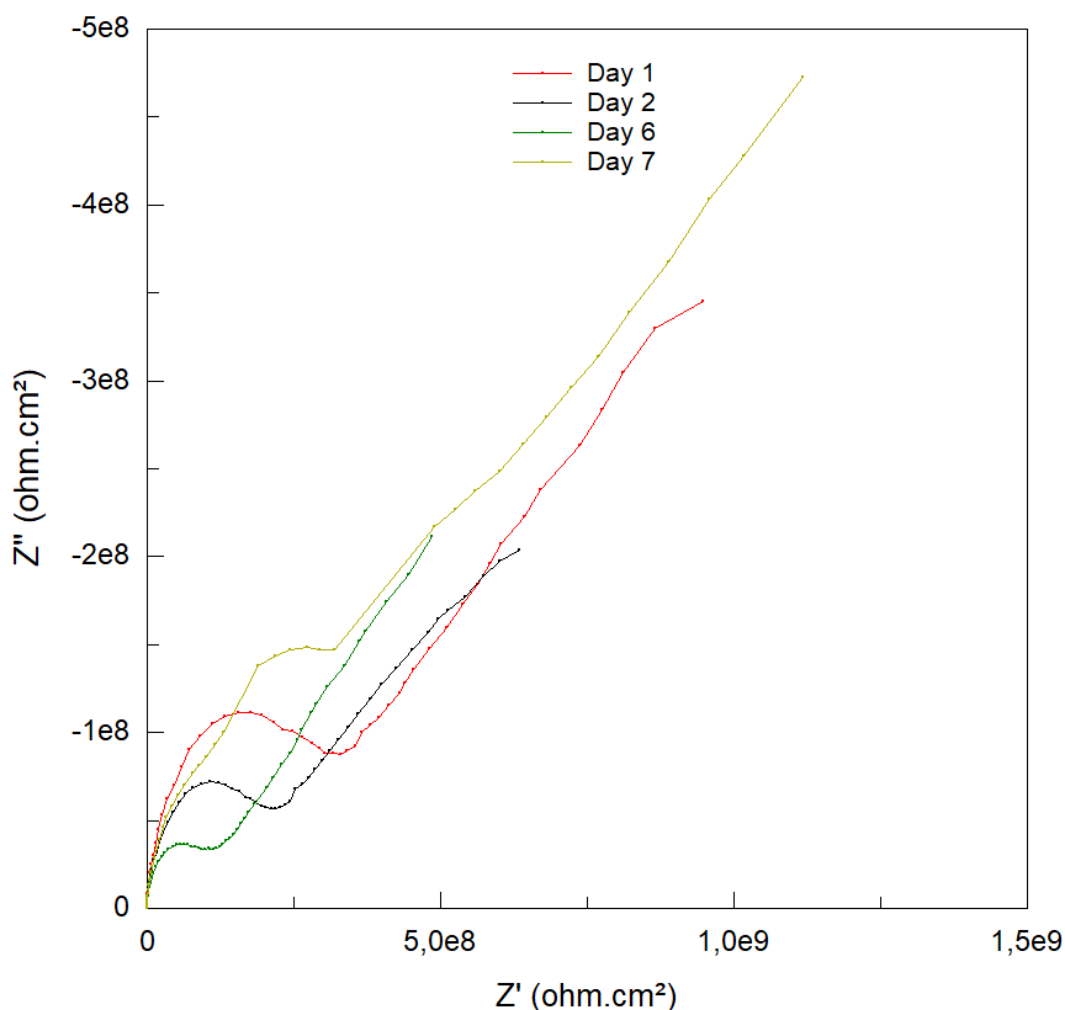


Figure 30 Nyquist plot using sodium phosphate as corrosion inhibitor

The first noticeable result is that the impedance response has greatly increased when an inhibitor has been used. The spectra reveal a loop at high frequency and then a slope that can be assigned to mass transport controlled phenomena. The inductive loop has disappeared. This low frequency process is due to mass transfer, of charged species, and the process is now mass controlled. Charged species take more time to pass through the protective layer created by the inhibitor and this slow down the corrosion rate over time.

The Bode plots shown in Figure 31 also provide useful insights.

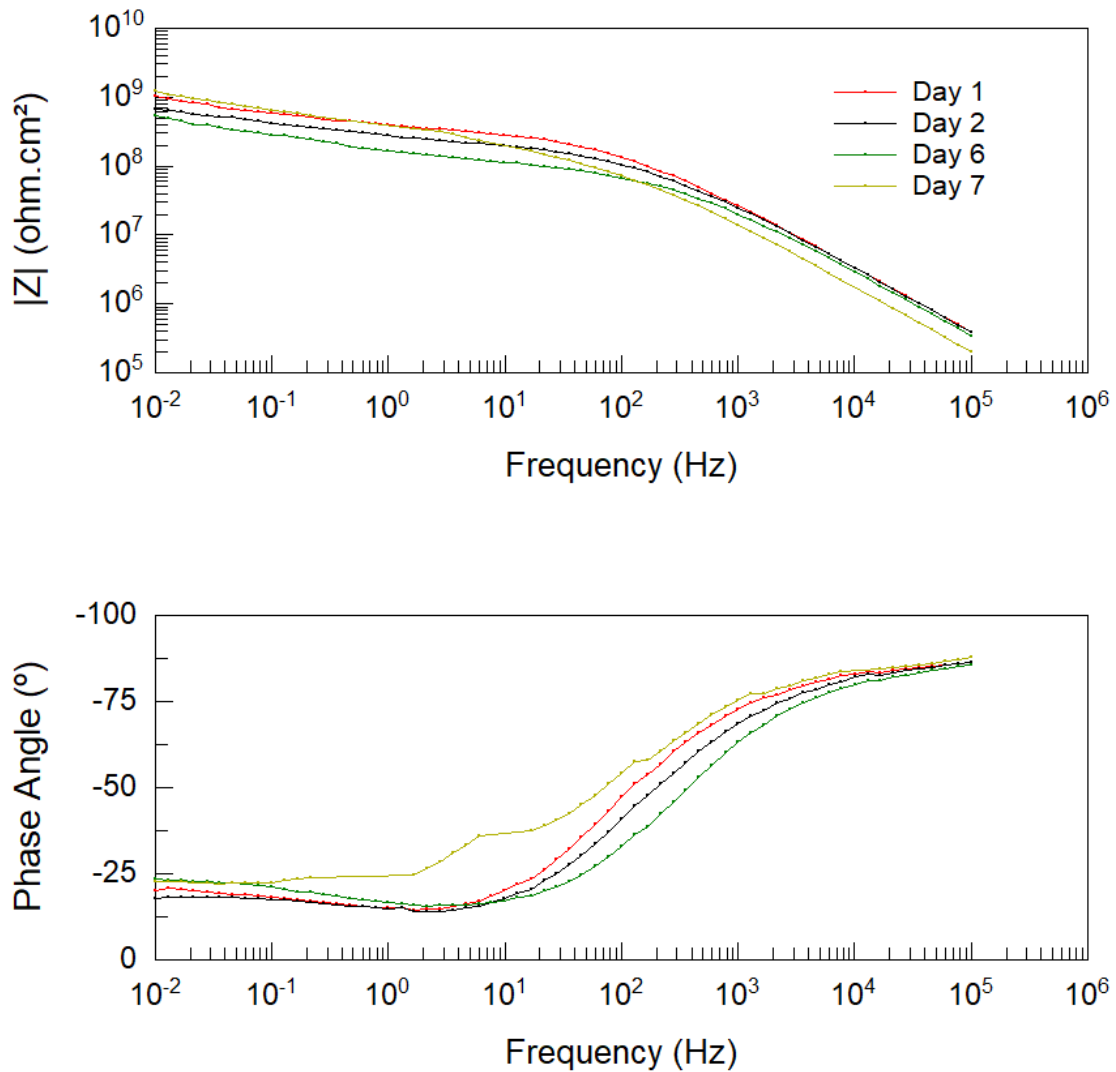


Figure 31 Bode plots using sodium phosphate as corrosion inhibitor

As observed this mass controlled effect contributed to increase significantly the impedance leading to impedance values almost 5 orders of magnitude above the ones without inhibitor. Moreover, the high frequency resistive response was no longer observed and from the very high frequencies a capacitive slope was observed, revealing the formation of a dense barrier layer that greatly protects the original bare metal, leading to very high resistances at the low frequency. This reveals that the inhibitor, which early accelerated corrosion (as suggested by the OCP evolution) leads to the formation a thick barrier layers that introduce a mass controlled corrosion process. In practical terms this would decrease the active area exposed to the electrolyte and would introduce diffusional effects in the response of the Mg anode over time.

Even though inhibitors typically increase impedance in the electrode when added in NaCl [29], [31], [32], [36], the combination of NaNO<sub>3</sub> and sodium phosphate shows a magnitude of

impedance that does not appear so far in the literature. A fast, thick, protective layer that introduces a mass controlled process that greatly increases the impedance that isolates the electrode and makes current flow more difficult.

## 4.4. Galvanostatic Discharge

### 4.4.1. Blank electrolyte results

This first set of chrono amperometry experiments (discharge curves) represent three different currents applied consecutively in the same sample, which was immersed 24 hours before the experiment was held in order to achieve an acceptable OCP stabilization. The currents applied to the electrode are 2.5, 5 and 10 mA respectively and are applied in this same order, from lower to the highest to avoid extra corrosion and unwanted reactions in the sample from the same beginning. The total area of the exposed sample had to be input in the used software, so the current mentioned in this paragraph is already divided by the area of the sample.

2 samples are tested after 24h of immersion in the blank electrolyte for each applied current. For comparative purposes a “fresh” sample was also prepared and submitted to the highest applied current. To discard the effect of consecutive polarizations at different current densities a sample immersed for 24 h was immediately subjected to the highest applied current.

Electrode materials that exhibit more negative discharge potential during the discharge test are able to supply higher voltage when serving as anodes in fully assembled Mg air batteries.

The results depicted in Figure 32 show that all the discharge potentials show a very sudden drop during the first 100 seconds and then the values stabilize keeping constant and between -1.1 and -1.4 V. This is characteristic of Mg air batteries and corresponds to the accumulation of discharge corrosion products at the electrode as soon as the current is imposed. No relevant changes were observed over time and, furthermore, the effect of the applied current do not have a significant effect on the potential of the electrode under applied current, as expected in typical Mg air batteries using NaCl [30], [31].

Interestingly, the fresh sample revealed a faster decay, probably due to the absence of the corrosion layer that was formed during the 24h immersion period. In practice the presence of this corrosion layer is the typical situation as the anode is expected to be in contact with the electrolyte even when the battery is not on.

Also, another conclusion is that the applied current do not affect the electrode voltage and the response is reliable even when increasing the applied current. This reveals that the electrode presents a stable electrochemical performance under different applied currents and that the voltage of the electrode remains stable in these various conditions.

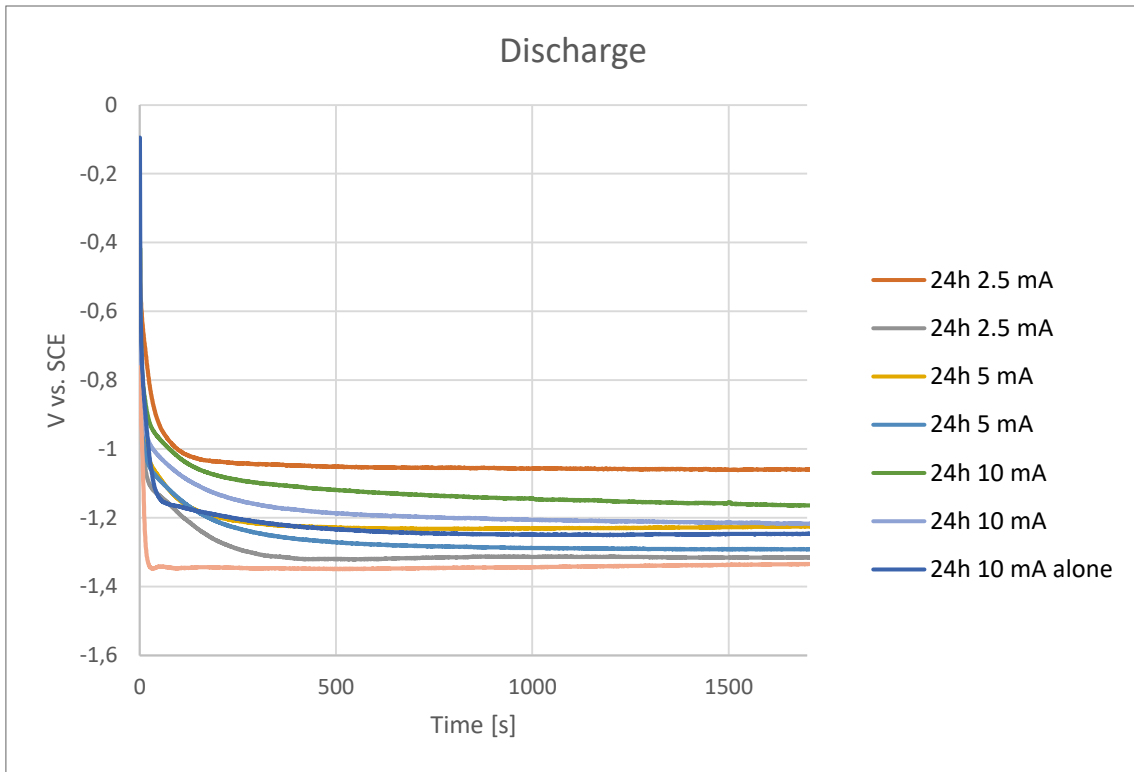


Figure 32 Galvanostatic discharge curves using blank electrolyte

#### 4.4.2. Results with inhibitor

A set of chronoamperometry experiments using different inhibitor concentrations is obtained at the current intensity of 2.5 mA. In order to see if the concentration amount of sodium phosphate would have any effect on the electrode discharge, the three different concentrations have been tested twice. All samples were immersed in the electrolyte with its respective inhibitor concentration 24 h before the test was done. This procedure allows the sample to stabilize and avoids any unwanted reactions that can hide the electrode response during chronoamperometry.

As it can be observed in Figure 33, the red curves correspond to a concentration of 0.01 M of sodium phosphate. The yellow and the blue curves correspond to a concentration of 0.005 M and 0.05 M respectively. Two samples of each concentration are plotted in order to check how behavior changes between concentrations and to see if the results of each concentration remain similar.

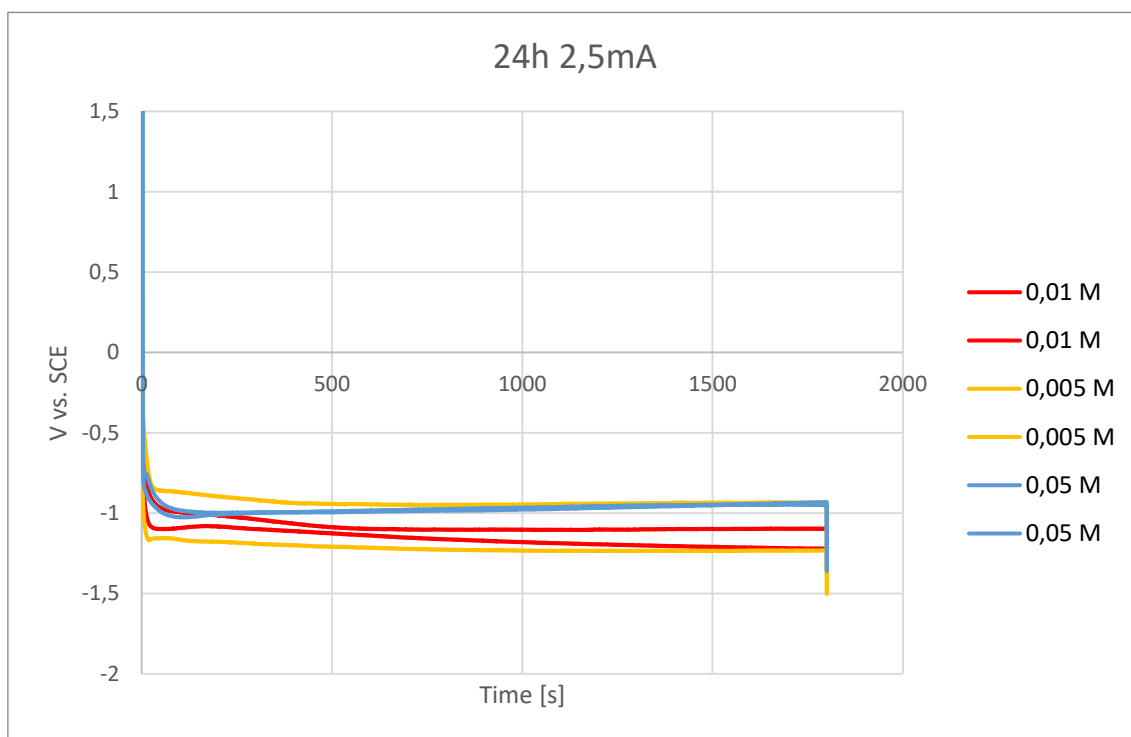


Figure 33 Discharge curves at 2.5 mA using different inhibitor concentrations

The results evidence a sudden decrease of the potential towards values slightly below -1.0 V and the inhibitor effect is not relevant. However, the general trend suggests that the two lowest concentrations induce slightly lower potentials, while the highest inhibitor concentration provides less negative values. Overall, it can be said that the presence of inhibitor, for the same applied current, decreases the electrode potential. This might be due to the fact that the inhibitor changes the corrosion process rate and mechanism. EIS have shown much higher impedances and mass transfer controlled reactions that might be responsible for the lowest potential of the electrode during discharge.

This is important because in the cell, the electrode potential can be affected by the charge transfer overpotential ( $\eta_{ct}$ ), by the diffusion overpotential ( $\eta_{diff}$ ) and by the  $iR$  drop ( $R$  is the electrolyte resistance). Since for all electrodes  $iR$  is the same (the same cell arrangement is used) the differences are related to the mechanism. In fact, it can be said that the diffusional polarization can reduce the final voltage of the Mg anode and this is more likely for the electrodes tested in the presence of the largest amount of inhibitor.

In order to see how different currents would affect the electrode response, discharge curves were obtained under currents of 5 mA and 10 mA.

The 0.05 M concentration of sodium phosphate was not further tested in the discharge curves. In Figure 34 the 0.01 M and 0.005 M concentrations were tested, each one of them at the two previously commented currents.

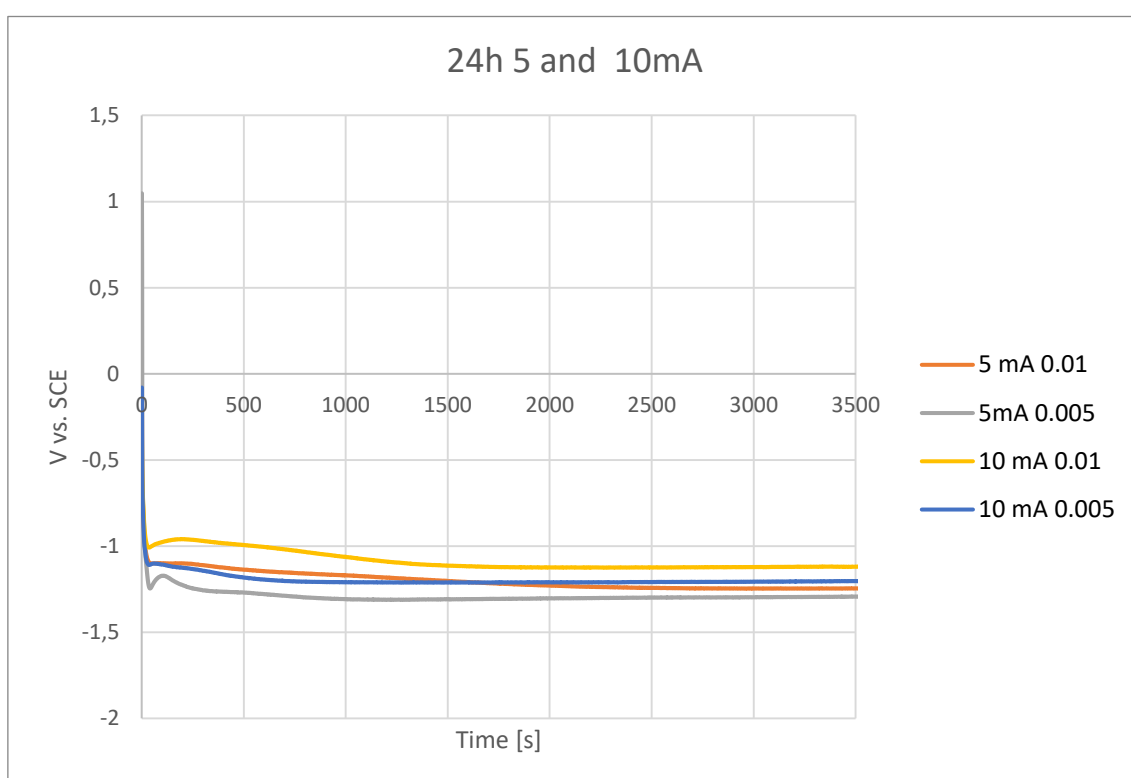


Figure 34 Discharge curves at 5 and 10 mA

The obtained curves are very similar to the curves corresponding to chronoamperometry experiments using blank electrolyte and the ones using different inhibitor concentrations, but a different current, which was 2.5 mA as previously commented.

Similarly to the previous results, the higher current densities do not affect the electrode potential under discharge and the values are constant and around -1.2 V.

From the experimental observations it can be assumed that the applied current density do not have any major effect on the discharge response of the Mg electrode, this is a common observation for sodium phosphate even when mixed with NaCl [29]



## 5. Conclusions

There main conclusions that can be extracted after finishing the experimental part:

- A  $\text{NaNO}_3$  electrolyte was chosen to evaluate the performance of a Mg AZ31 anode in the absence and presence of sodium phosphate as corrosion inhibitor. This is a new approach compared to the actual state of art.
- There is a significant decrease in OCP from the samples that were naturally immersed in an aqueous solution of  $\text{NaNO}_3$  compared to the ones that were immersed in an electrolyte that contains sodium phosphate as an inhibitor. A lower OCP suggests that the overall potential of the cell will be higher.
- The discharge voltage remains similar for the different applied currents. Even though different concentrations and different currents were tested, there is no evidence that any of the parameters tried can have a significant impact on the resulting discharge curves. This evidences good stability of the electrode even under high current demands an effect that can be advantageous for the Mg air battery.
- There is a very important increase in the impedance when the inhibitor is added to the electrolyte. Visually it can also be seen the rapid formation of a passivation layer that blocks the active areas of the electrode changing the mechanism to a mass controlled condition. This increases the diffusion overpotential that, in turn decreases the electrode potential. Both these factors may have a negative impact on the electrode resistance and current response in the presence of the largest concentration of sodium phosphate as inhibitor.
- Although d.c. polarization (faster experiment) did not evidence relevant mechanism changes in the Mg electrodes in the presence and absence of inhibitor, thanks to electrochemical impedance spectroscopy (EIS), a resistive electrode was formed accompanied by mass transfer control. This can slowdown the response of the electrode compared to a condition using lower inhibitor concentrations. This may also affect the time response of the anode.
- After studying the effect of three different concentrations, 0.01 M of sodium phosphate is found to be a good concentration to be further tested in this project, mainly due to the lower OCP obtained in the potentiodynamic polarization and open circuit potential experiments. It is also observed that 0.005 M shows decent potential and reliable discharge curves, making it a plausible option prior to further experiments.
- Even though the usage of 0.01 M sodium phosphate seemed to have some beneficial aspects, the very large increase of low frequency impedance might make the usage of these inhibitor unsuitable for commercial purposes. Further experiments should be held in order to see how this would affect the final battery and its viability.

## 6. Future work

After finishing the experiments, analyzing the results and extracting some conclusions it is clear that more research needs to be done, especially because Mg air batteries still have a lot of potential to improve its performance and characteristics. Some of the points that should follow this work are:

- Test in more detail EIS of all inhibitor concentrations and enlarge the range of concentrations to be studied
- Test different inhibitors
- Assemble a cell and run discharge curves and calculate both capacity and capacity retention under different current densities.
- Determine the capacity and resistance over the time in presence and absence of inhibitor

## 7. References

- [1] "WEO 2018." [Online]. Available: <https://www.iea.org/weo2018/>. [Accessed: 23-Jun-2019].
- [2] H. Abolhosseini, A. Heshmati, and J. Altmann, "A review of renewable energy supply and energy efficiency technologies," *IZA Discuss. Pap. Ser.*, no. 8145, pp. 1–36, 2014.
- [3] H. Horie, "Research and Development Work on Advanced Lithium-Ion Batteries for High-Performance Environmental Vehicles," *Lithium Ion Recharg. Batter. Mater. Technol. New Appl.*, vol. 1, pp. 313–327, 2010.
- [4] Jérôme Duval, "África | La fiebre del cobalto en el Congo - El Salto - Edición General." [Online]. Available: <https://www.elsaltodiario.com/africa/fiebre-cobalto-congo-mineria-china-glencore>. [Accessed: 30-Sep-2019].
- [5] M. Sedacca, "Better batteries," *Sci. Am.*, vol. 317, no. 4, p. 23, 2017.
- [6] Y. Miao, P. Hynan, A. Von Jouanne, and A. Yokochi, "Current li-ion battery technologies in electric vehicles and opportunities for advancements," *Energies*, vol. 12, no. 6, pp. 1–20, 2019.
- [7] G. J. May, A. Davidson, and B. Monahov, "Lead batteries for utility energy storage: A review," *J. Energy Storage*, vol. 15, pp. 145–157, 2018.
- [8] K. R. Bullock, "Lead/acid batteries," *J. Power Sources*, vol. 51, no. 1–2, pp. 1–17, 1994.
- [9] R. Kasim, A. R. Abdullah, N. A. Selamat, M. S. S. M. Basir, and M. Z. Ramli, "Nickel-Cadmium battery analysis using spectrogram," *ARPN J. Eng. Appl. Sci.*, vol. 11, no. 6, pp. 3975–3979, 2016.
- [10] P. Bernard and M. Lippert, *Nickel-Cadmium and Nickel-Metal Hydride Battery Energy Storage*. Elsevier B.V., 2014.
- [11] Z. Wen, J. Cao, Z. Gu, X. Xu, F. Zhang, and Z. Lin, "Research on sodium sulfur battery for energy storage," *Solid State Ionics*, vol. 179, no. 27–32, pp. 1697–1701, 2008.
- [12] R. Carnegie, D. Gotham, D. Nderitu, and P. V Preckel, "Utility scale energy storage systems- Benefits, application and technologies," no. June, p. 95, 2013.
- [13] B. M. S. Whittingham, "History, Evolution and Future Status of Energy Storage," vol. 100, 2012.
- [14] P. Leung, X. Li, C. Ponce De León, L. Berlouis, C. T. J. Low, and F. C. Walsh, "Progress in redox flow batteries, remaining challenges and their applications in energy storage," *RSC Adv.*, vol. 2, no. 27, pp. 10125–10156, 2012.
- [15] M. C. Kocer *et al.*, "Assessment of battery storage technologies for a Turkish power network," *Sustain.*, vol. 11, no. 13, 2019.
- [16] Y. Li and J. Lu, "Metal-Air Batteries: Will They Be the Future Electrochemical Energy Storage Device of Choice?," *ACS Energy Lett.*, vol. 2, no. 6, pp. 1370–1377, 2017.
- [17] N. Nitta, F. Wu, J. T. Lee, and G. Yushin, "Li-ion battery materials : present and future," *Biochem. Pharmacol.*, vol. 18, no. 5, pp. 252–264, 2015.
- [18] C. Wang *et al.*, "Recent progress of metal-air batteries-A mini review," *Appl. Sci.*, vol. 9, no. 14, pp. 1–22, 2019.

- [19] B. Diouf and R. Pode, "Potential of lithium-ion batteries in renewable energy," *Renew. Energy*, vol. 76, pp. 375–380, 2015.
- [20] T. Zhang, Z. Tao, and J. Chen, "Magnesium-air batteries: From principle to application," *Mater. Horizons*, vol. 1, no. 2, pp. 196–206, 2014.
- [21] X. Zhang, X. Wang, Z. Xie, and Z. Zhou, "ScienceDirect Recent progress in rechargeable alkali metal e air batteries," *Green Energy Environ.*, pp. 1–14, 2016.
- [22] A. R. Mainar *et al.*, "An overview of progress in electrolytes for secondary zinc-air batteries and other storage systems based on zinc," *J. Energy Storage*, vol. 15, pp. 304–328, 2018.
- [23] Y. Li and H. Dai, "Recent advances in Zinc-air batteries," *Chem. Soc. Rev.*, vol. 43, no. 15, pp. 5257–5275, 2014.
- [24] J. Ma, G. Wang, Y. Li, F. Ren, and A. A. Volinsky, "Electrochemical performance of Mg-air batteries based on AZ series magnesium alloys," *Ionics (Kiel)*, vol. 25, no. 5, pp. 2201–2209, 2019.
- [25] Y. Sun *et al.*, "Recent advances and challenges in divalent and multivalent metal electrodes for metal–air batteries," *J. Mater. Chem. A*, vol. 7, no. 31, pp. 18183–18208, 2019.
- [26] R. Mohtadi and F. Mizuno, "Magnesium batteries: Current state of the art, issues and future perspectives," *Beilstein J. Nanotechnol.*, vol. 5, no. 1, pp. 1291–1311, 2014.
- [27] R. Zhang, O. Tutusaus, R. Mohtadi, and C. Ling, "Magnesium-sodium hybrid battery with high voltage, capacity and cyclability," *Front. Chem.*, vol. 6, no. DEC, pp. 1–10, 2018.
- [28] F. W. Richey, B. D. McCloskey, and A. C. Luntz, "Mg anode corrosion in aqueous electrolytes and implications for Mg-air batteries," *J. Electrochem. Soc.*, vol. 163, no. 6, pp. A958–A963, 2016.
- [29] Y. Li, J. Ma, G. Wang, F. Ren, Y. Zhu, and Y. Song, "Investigation of sodium phosphate and sodium dodecylbenzenesulfonate as electrolyte additives for AZ91 magnesium-air battery," *J. Electrochem. Soc.*, vol. 165, no. 9, pp. A1713–A1717, 2018.
- [30] D. Höche *et al.*, "Performance boost for primary magnesium cells using iron complexing agents as electrolyte additives /639/638/675 /639/301/299/161/891 /128 /123 /132 article," *Sci. Rep.*, vol. 8, no. 1, pp. 1–9, 2018.
- [31] Y. C. Zhao, G. S. Huang, G. L. Gong, T. Z. Han, D. B. Xia, and F. S. Pan, "Improving the intermittent discharge performance of Mg-air battery by using oxyanion corrosion inhibitor as electrolyte additive," *Acta Metall. Sin. (English Lett.)*, vol. 29, no. 11, pp. 1019–1024, 2016.
- [32] M. A. Deyab, "Decyl glucoside as a corrosion inhibitor for magnesium-air battery," *J. Power Sources*, vol. 325, pp. 98–103, 2016.
- [33] S. You, Y. Huang, K. U. Kainer, and N. Hort, "Recent research and developments on wrought magnesium alloys," *J. Magnes. Alloy.*, vol. 5, no. 3, pp. 239–253, 2017.
- [34] R. Hydrogen and E. Rhe, "What are Normal Hydrogen Electrode ( NHE ), Standard Hydrogen Electrode What are Normal Hydrogen Electrode ( NHE ), Standard Hydrogen Electrode ( SHE ) and Reversible Hydrogen Electrode ( RHE )?," no. January, 2019.
- [35] T. Zheng, Y. Hu, and S. Yang, "Effect of grain size on the electrochemical behavior of

- pure magnesium anode," *J. Magnes. Alloy.*, vol. 5, no. 4, pp. 404–411, 2017.
- [36] S. V. Lamaka, B. Vaghefinazari, D. Mei, R. P. Petrauskas, D. Höche, and M. L. Zheludkevich, "Comprehensive screening of Mg corrosion inhibitors," *Corros. Sci.*, vol. 128, no. September, pp. 224–240, 2017.
- [37] S. A. Salman, R. Ichino, and M. Okido, "A comparative electrochemical study of AZ31 and AZ91 magnesium alloy," *Int. J. Corros.*, vol. 2010, pp. 1–8, 2010.
- [38] K. M. Ismail and S. Virtanen, "Electrochemical behavior of magnesium alloy AZ31 in 0.5 M KOH solution," *Electrochem. Solid-State Lett.*, vol. 10, no. 3, pp. 2006–2008, 2007.
- [39] J. Genescà Ferrer and J. Juárez, "Development and testing of galvanic anodes for cathodic protection," *Contrib. to Sci.*, vol. 1, no. 3, pp. 331–343, 2000.

## Annex

### A.1. Open circuit potential

The results show all the points measured in the first 24 hours of the sample's immersion. In order to appreciate more the behavior in the beginning of the immersion, where more points are concentrated, the following graphs show different time intervals:

Figure 35, which shows the first 600 seconds, indicates us that right after immersion an OCP of almost -1.6 V was obtained and during this time lapse it increased until -1.53 V.

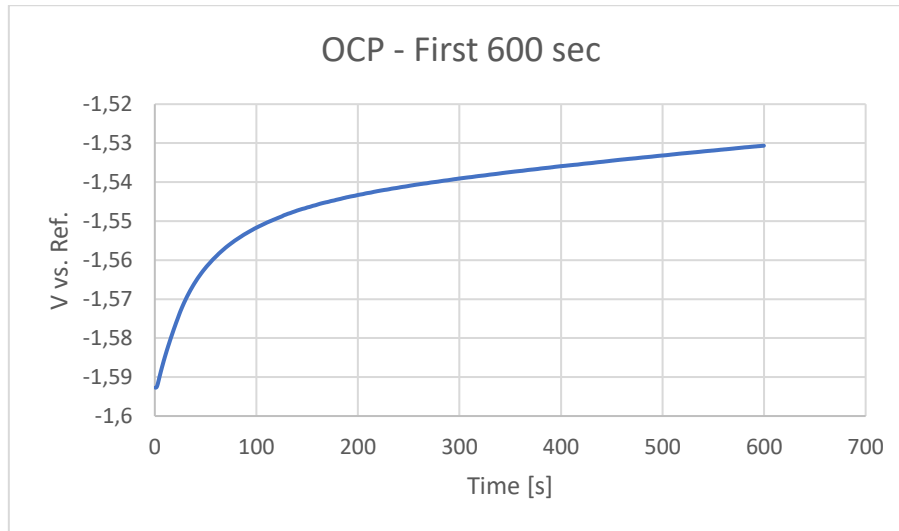


Figure 35 OCP first 600 seconds

Figure 36 shows the behavior of the sample during the first hour, but excluding the first 600 seconds, that are shown in the previous graph. It is clear that the tendency is that the OCP is still increasing over time, from -1.53 V until -1.485 V, although this tendency is now clearly linear instead of logarithmic.

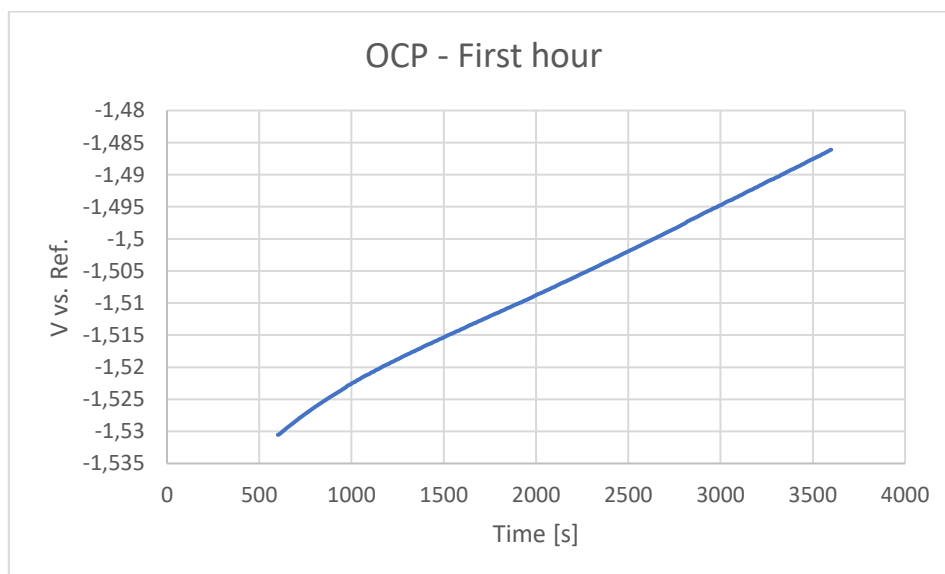


Figure 36 OCP first hour